CHAPTER 3

CATALYST CHARACTERIZATION

CHAPTER 3 : CATALYST CHARACTERIZATION

3.1 Introduction

Catalyst characterization is very important as most practical catalysts are highly complex materials. To characterize a polymer-bound catalyst precisely, the constitution of the catalyst has to be understood in its bulk as well as on its surface mainly surface composition and nature and proportion of surface functional groups. We also require to know the modification of the polymer during different stages of its preparation; swelling behaviour of the catalyst and change in thermal stability. In addition, we ought to understand the structure of the catalyst i.e. geometric structure and morphology particularly change in morphology by supporting on polymer. Finally characterization should be carried out in terms of catalytic activity which is a quantitative measurement of the ability of the catalyst to carry out a particular chemical transformation under specified condition (1).

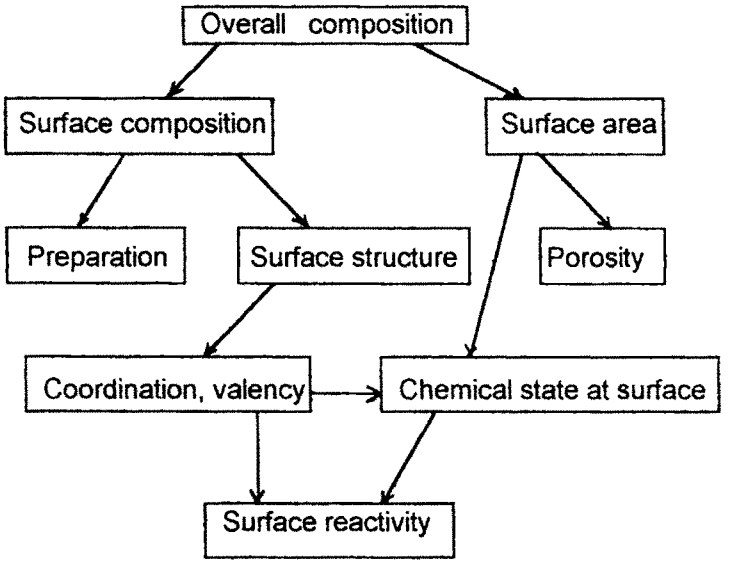

Fig.3.1 General scheme of characterization (1).

Present chapter deals with characterization of polymer-bound catalysts as also that of unbound transition metal complexes. An attempt has been made to arrive at surface composition and catalyst structure using different means of characterization viz. elemental analyses, swelling studies, investigation of moisture content and apparent bulk density as well as measurement of surface area. Spectroscopic analyses such as infrared and reflectance UV-visible spectra, electron spin resonance (ESR), electron spectroscopy for chemical analysis (ESCA or XPS) were carried out in order to investigate co-ordination structure of anchored complexes and oxidation state of metal atom. Morphology of the supports and catalysts was studied using scanning-electron microscope (SEM) while the thermal stability was investigated using thermogravimetric (TG) analysis. Based on the spectroscopic and physico-chemical characteristics, the probable structures of metal complexes on the polymer matrices have been proposed. The catalytic activity of the catalysts has been investigated for the hydrogenation of 1-hexene and styrene, and oxidation of benzyl alcohol.

3.2 Apparent bulk density and moisture content

Apparent bulk density and percentage of moisture of all polymer supports and catalysts are given in Table 3.1. Bulk density and percentage moisture content of the catalysts were found to increase with an increase in percentage cross-linking of the polymer support. Moisture content of Ruthenium catalysts were found to be more than that of palladium catalysts. Since the polymer support P(S-DVB) is hydrophobic in nature (2), the similar nature of the supported catalysts may be attributed either due to hydrogen bonding of water with amino groups or co-ordination with metal atom.

Table 3.1

Moisture content and apparent bulk density of polymer supports and catalysts

	Moisture content (wt %)	Apparent bulk density (g ml^{-1})
- *Support (cross-linking)*		
XAD-2 (2%)	0.350	0.380
AM-44 (8%)	0.280	0.390
AM-24 (14%)	0.310	0.390
- *Catalyst*		
A = 2PRu(III)Salen	0.353	0.380
B = 2PPd(II)Salen	0.350	0.380
C = 8PRu(III)Salen	1.039	0.428
D = 8PPd(II)Salen	0.829	0.476
E = 14PRu(III)Salen	1.608	0.419
F = 14PPd(II)Salen	1.028	0.421
G = 8PPd(II)EDTA	0.96	0.427
H = 8PRu(III)EDTA	1.290	0 417
I = 14PPd(II)EDTA	1.120	0.388

The importance of apparent bulk density lies in indication of mass of catalyst that can be packed into a specified volume of reactor. However, volume occupied by swollen polymer is different than that occupied by dry polymer. Therefore this parameter is not significant when catalyst is used in liquid phase slurry reactor but useful for vapour phase reactor.

3.3 Surface area measurement

Most practical catalysts are highly complex materials and a basic problem is how to correlate catalyst behaviour with physical and chemical structure. Some methods of characterization are standardized. These include determination of total surface area. Measurement and comparison of surface area of catalyst supports and the catalysts give an idea about a change in surface area upon immobilization or anchoring of support and also relation between change in activity and change in surface area. Adsorption method was used for the measurement of total surface area of polymer supports and polymer-

bound catalysts (3). Adsorption - desorption isotherms of nitrogen were recorded on a Carlo-Erba Sorptiomatic series-1900 at liquid N_2 temperature (i.e. -196°C), after degassing the sample at 80°C for 4 hours. From the isotherms, specific surface area and pore volume were calculated using BET equation. The results are given in table 3.2. In some cases a decrease in surface area was observed while in some other cases an increase was found after the complex formation (Table 3.2). A decrease observed in the surface area of some of the catalysts may be due to blocking of pores of the support by successive introduction of chloromethyl groups, schiff base ligand and metal on the polymer matrix. This is in accordance with the results obtained earlier by Ram et al (4-6). While an increase may be attributed due to complexing of highly functionalized polymer (extent of chloromethylation 17.5% for AM-44 beads) with bulky ligands (7).

3.4 Chemical composition

Elemental analysis of C, H, N, Cl and metal content for polymer-bound Ru and Pd complexes at various stages of preparation of the catalysts are given in Tables 3.3-3.4. The number of ligand molecules attached with the polymer were calculated from difference of two chloride ion contents (estimated gravimetrically) before and after introduction of ligand. The calculated and experimental values were found to be in close agreement. Low loading of the metal and hence the chelation on the polymer matrix was achieved by carrying out the complexation reaction under mild conditions in presence of a good swelling agent. It is obvious that the polymer complex formation represents a complicated process. The polymer matrix swells after absorbing the solvent which changes the polymer structure. The swollen polymer then interacts with the metal ions and the complex formation takes place. It may be taken into account that each functional group or ligand comes in contact with metal ions and coordinates with this to form inner co-ordination complex. Then the spatial arrangement of the complexing groups over the

polymer ligand chain takes various concentrations with respect to the main chain. As a result, the total polymer complex as a whole is formed. The polymer complex formation also represents relaxation process which is related to the probability of transition of the system from one state of equilibrium to another (8)

Table 3.2

Surface area and pore volume of polymer supports and catalysts

	Surface area (m^2g^{-1})	Pore volume ($cm^3\ g^{-1}$)
- *Supports (cross-linking)*		
XAD-2 (2%)	330.00	0.420
AM-44 (8%)	37.37	0.043
AM-24 (14%)	62.03	0.098
- *Catalysts*		
A = 2PRu(III)Salen	222.06	0.464
B = 2PPd(II)Salen	230.87	0.589
C = 8PRu(III)Salen	43.76	0.146
D = 8PPd(II)Salen	44.44	0.092
E = 14PRu(III)Salen	75.69	0.279
F = 14PPd(II)Salen	57.40	0.156
G = 8PPd(II) EDTA	44.08	0.147
H = 8PRu(III) EDTA	21.28	0.083
I = 14PPd(II) EDTA	85.26	0.396

Table 3.3

Elemental analyses at different stages of preparation of polymer-bound Ruthenium complexes (wt%)

Catalyst	X			Y			Z			
	C	H	Cl	C	H	N	C	H	N	Ru
A	63.06	7.62	5.30	80 39	6 52	1.64	82 50	6 98	1 34	$2\ 72x10^{-3}$
C	68 95	5 93	17 50	63 17	6 02	3 67	61.56	6 88	4 51	$7\ 12x10^{-2}$
E	80.84	7 42	4 70	82.86	7 26	2 84	85.69	7 11	<1	$2\ 97x10^{-3}$
H	68.95	5 93	17 50	69 58	6 10	1 30	70 42	6.47	<1	$4.95x10^{-4}$

Table 3.4

Elemental analyses at different stages of preparation of polymer-bound palladium complexes (in wt %)

Catalyst	X			Y			Z			
	C	H	Cl	C	H	N	C	H	N	Pd
B	63.06	7.62	5.30	80 39	6.52	1.64	82 21	6.63	1 34	$9\ 57\times10^{-2}$
D	68.95	5.93	17.50	63.13	6.02	3.67	60.95	6 06	2.65	$1\ 16\times10^{-3}$
F	80.84	7 42	4.70	82 86	7.26	2.84	82 13	7 52	<1	$0\ 45\times10^{-3}$
G	68 95	5.93	17 50	69.58	6.10	1 30	68 59	6.69	<1	$3\ 2\times10^{-3}$
I	80 84	7.42	4.70	69.58	6.10	1 18	86.16	6 97	<1	$2\ 8\times10^{-3}$

3.5 Swelling studies

The interaction of polymers with low molecular mass solvents, resulting in limited or unlimited swelling, has long been the subject of investigation from theoretical and practical points of view (9). The swelling theory was formulated many years ago and has been developed more recently (10). There has been notable efforts to find a relation between swelling behaviour and structural parameters, such as extent of cross-linking of polymer network. In catalysis by polymer-bound complexes, swelling is a very useful parameter.

Higher activity and selectivity can be achieved with a polymer-bound catalyst, if the reactant molecules are accessible to all catalytic sites both on the surface and interior of the beads. This can be achieved by using a solvent in which the polymer has maximum swelling so that the matrix expands sufficiently to allow the reactant molecules to diffuse within the solvent channel and encounter the catalytic centers.

The extent of swelling depends on the polymer-solvent interaction which is determined by (i) the nature of the solvent and the polymer matrix and (ii) reactive groups attached to the polymer matrix.

Thus, nature of the solvent plays an important role in the rate of reaction. Polymer swelling is a very useful parameter to control both specificity and selectivity in a batch reactor. However, it becomes undesirable in a fixed bed reactor as it leads to blocking of the inter bead channels and so prevents flow through reactor bed.

In the present investigation, an attempt is made to ensure that the metal complexes are anchored uniformly during the synthesis and all catalytic centers are accessible during the reaction by carrying out an exhaustive study of swelling of the polymer support and catalysts using eleven different solvents of different nature (i.e aliphatic, aromatic, polar and non-polar. The results are given in Tables 3.5 to 3.7. The plot of polymer cross-link vs mole percent of swelling is given in figs. 3.2 to 3.4 for polymer supports and catalysts. It was observed that swelling decreases with increase in polymer-cross link in all cases. It was found that the affinity of the polymer matrix for different solvent changes when functional groups and metal atoms are incorporated into it Swelling decreases as the solvent nature is changed from polar to non-polar. Thus the maximum swelling of the catalysts was found to be with water while with n-hexane it was observed to be minimum. The maximum swelling in water may be due to hydrogen bonding of water molecules with amino groups. However, for the sake of comparison of catalytic activity of all the catalysts, a common solvent methanol is chosen as the reaction medium as in addition to better swellability it also offers miscibility of the substrates used.

Table 3.5

Swelling of the polymer supports studied using different solvents

Solvent	Swelling (mol %)		
	XAD-2 (2%)	AM-44 (8%)	AM-24 (14%)
Water	4.20	4.03	3.83
Methanol	3.12	2.72	2.30
Ethanol	2.20	1.98	1.78
Dioxane	1.84	1.54	1.32
N,N-dimethyl formamide (DMF)	1.52	1.27	1.13
Acetone	1.37	1.10	1.02
Tetrahydrofuran (THF)	1.06	1.00	0.91
Benzene	0.88	0.68	0.57
n-hexane	0.72	0.52	0.48

Table 3.6

Swelling of polymer supported Pd(II) catalysts in different solvents

	Swelling (mol %)				
Catalyst / solvent	2PPd(II)Salen	8PPd(II)Salen	14PPd(II)Salen	14PPd(II)EDTA	8PPd(II)EDTA
Water	4 65	4 05	3.48	3 27	3 71
Methanol	2.37	2.18	2.02	1 70	2 31
Ethanol	1 98	1 78	1 54	1 37	1 59
Dichloromethane (DCM)	1 34	1.20	1 06	1 23	1 43
N,N dimethyl formamide (DMF)	1 24	1.12	1.06	1 26	1 40
Tetrahydrofuran (THF)	1 12	1.02	0 94	1 13	1 35
Dioxane	1.53	0.92	1 08	1 06	1 21
Acetone	1.07	0 82	1.16	1 17	1 27
Benzene	1.06	0 98	0 88	1 05	1 29
Cyclohexane	0 75	0 59	0 46	0.58	0 76
n-hexane	0.62	0.56	0.44	0 52	0.62

Table 3.7

Swelling of polymer supported Ru(III) catalysts in different solvents

	Swelling (mol %)			
Catalyst / solvent	2PRu(III)Salen	8PRu(III)Salen	14PRu(III)Salen	8PRu(III)EDTA
Water	5.11	4.65	4.20	5.05
Methanol	2.20	2.02	1.91	4.53
Ethanol	1.60	1.45	1.39	2.80
Dichloromethane	1.46	1.41	1.31	2.68
N,N dimethyl formamide (DMF)	1.20	1.16	1.04	2.37
Dioxane	1.03	0.98	0.90	2.11
Tetrahydrofuran (THF)	0.89	0.88	0.78	1.55
Acetone	0.86	0.83	1.12	2.18
Benzene	0.84	0.82	0.66	0.92
Cyclohexane	0.65	0.59	0.48	0.61
n-hexane	0.55	0.45	0.34	1.19

3.6 Spectral Characterization

3.6.1 UV-visible spectroscopy

The interaction of light with catalyst particles is regarded as a major tool in the characterization of catalysts. The transitions involved in the UV-visible region are electronic. d-d transitions are observed when degenerate d orbitals are split by placing a transition metal ion in a crystal field. The splitting of the energy levels is affected by the number of d electrons, the effective charge on the ion, the distribution and the charge of the surrounding ions. These transitions usually occur in the visible part of the spectrum. Charge transfer transitions involve more than one atom and include transitions from metal to ligand or vice versa, or between two neighbouring metal atoms of different oxidation states. Usually such transitions occur in the UV region and do not mask the d-d transition in the visible region. The technique employed in the UV-visible spectroscopy for powdered samples involve the measurement of diffusely reflected light (11). In supported catalysis,

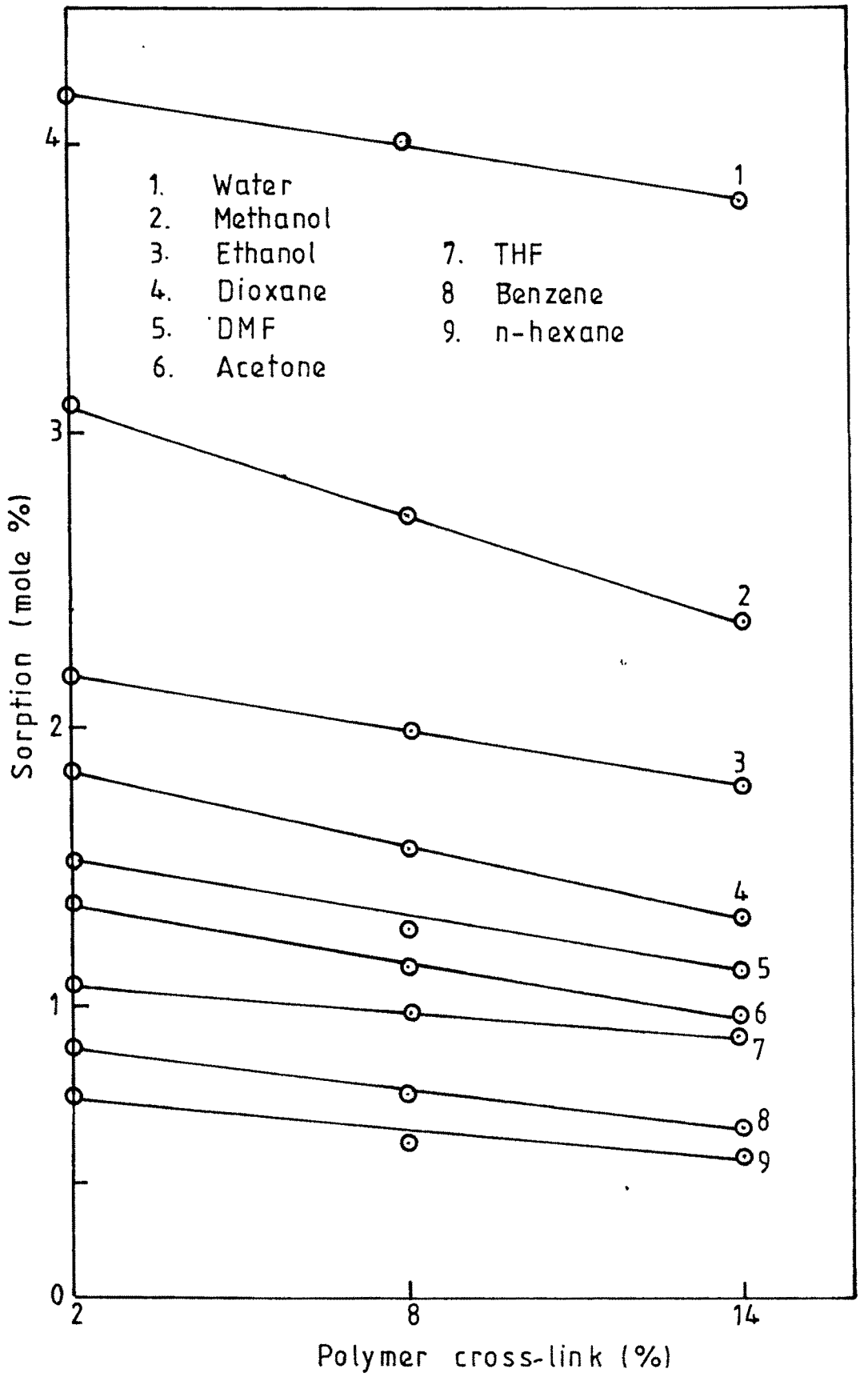

Fig. 3.2 Swelling studies of polymer supports

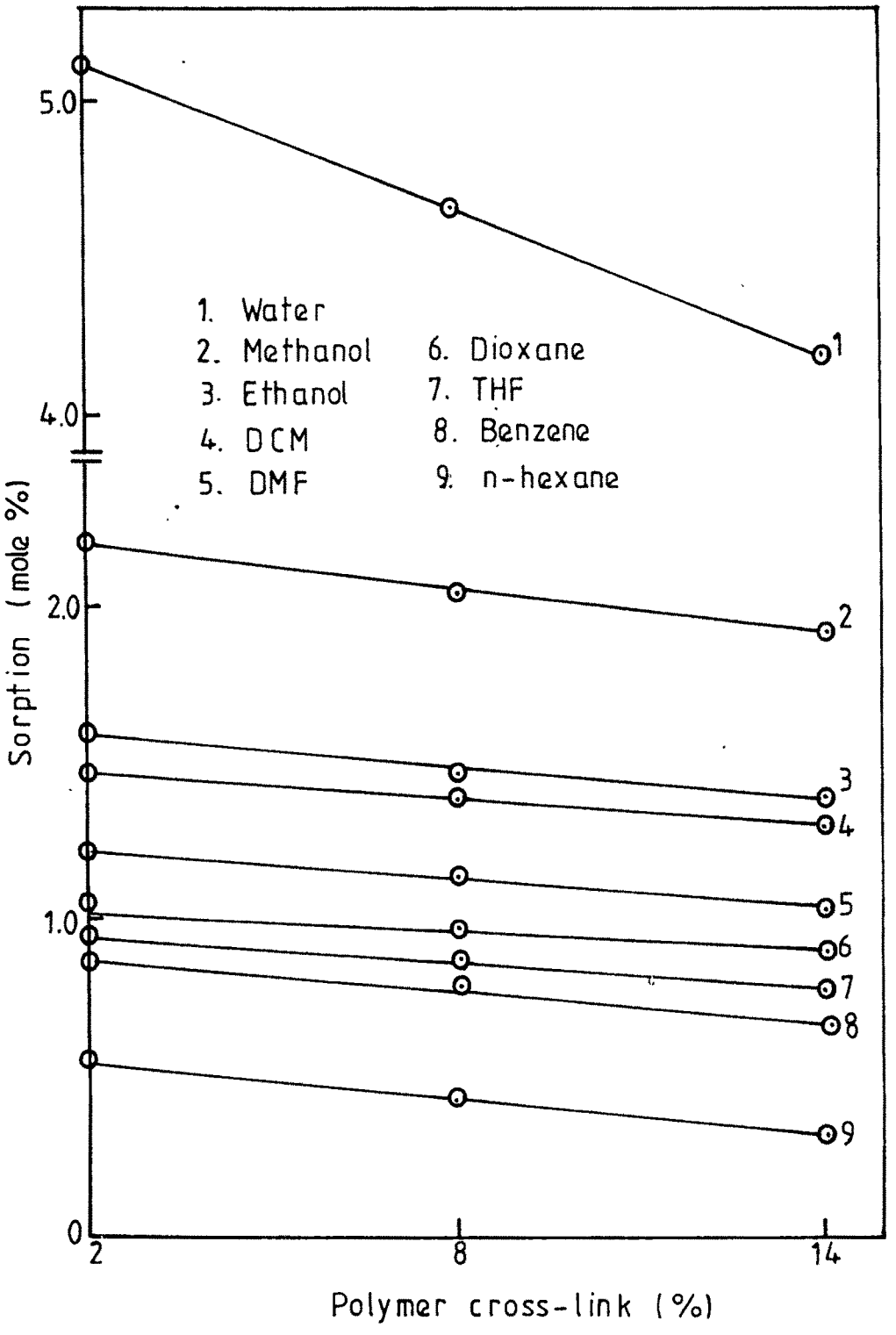

Fig. 3.3 Swelling studies of polymer supported ruthenium catalysts

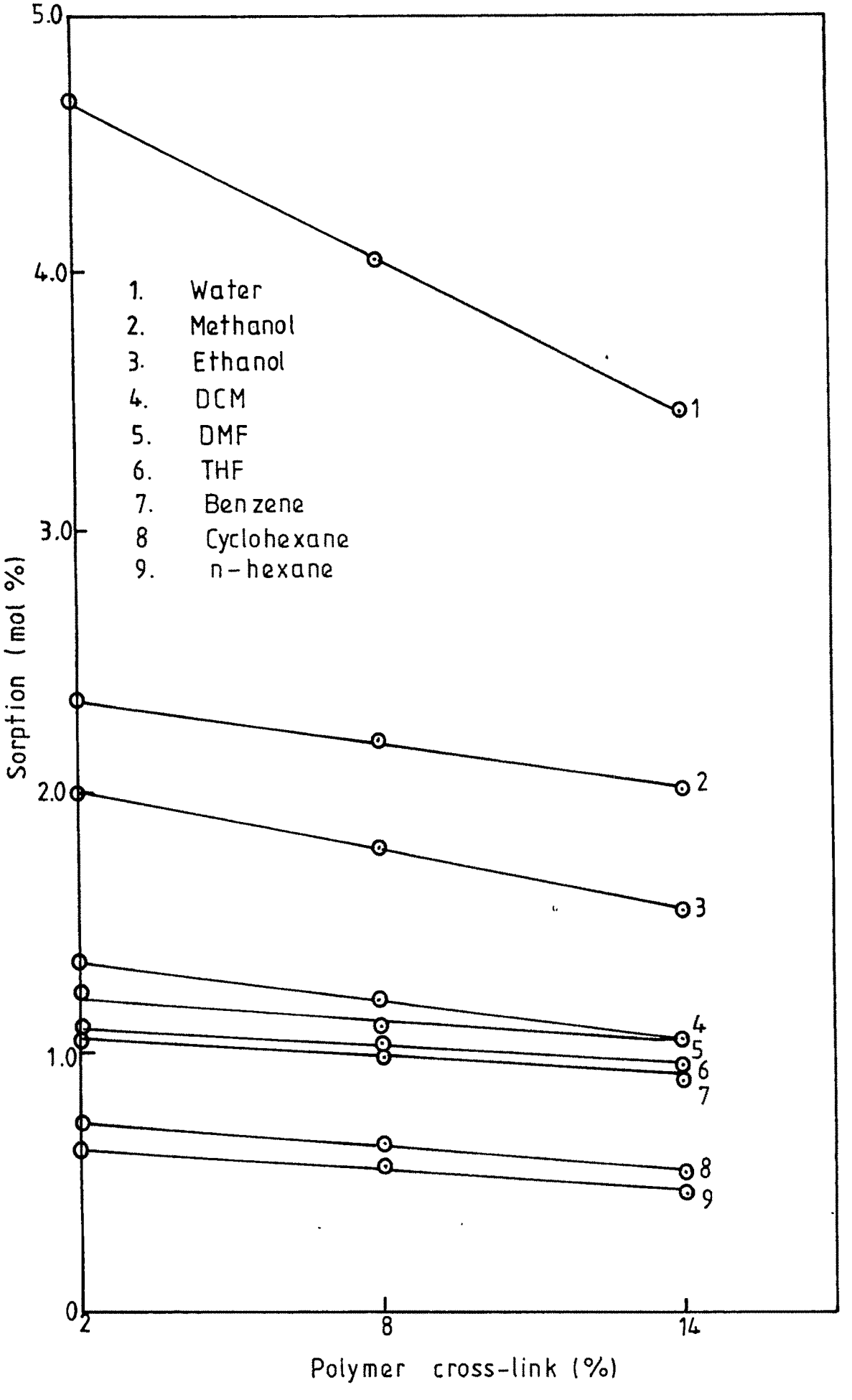

Fig. 3.4 Swelling studies of polymer supported palladium catalysts

UV-visible spectra are normally interpreted by comparison with the spectra of corresponding homogeneous complex. Figs. 3.5 and 3.7 show the UV-visible diffuse reflectance spectra of polymer-bound ruthenium and palladium catalysts using $BaSO_4$ as standard. Polymer-bound palladium catalysts show peak at 400 nm which might be due to d-d transitions of Pd(II). The homogeneous palladium schiff base complex also shows a peak at 400 nm confirming that palladium is present in same oxidation state both in heterogenized and homogeneous systems. The broad peak observed between 360 and 430 nm in case of polymer-bound ruthenium catalysts might be due to d-d transitions of Ru(III).

3.6.2 Infrared spectroscopy

Infrared spectroscopy is most widely used technique for the study of supported metal complex catalysts. It is used to study adsorbed molecules and their binding with catalyst surface. It provides reliable information about the organic compounds in the IR (600-4000 cm^{-1}) region and that of metal-ligand vibrations in Far-IR (50-600 cm^{-1}) region. The bond formed between the metal atom and the co-ordinating atom of the ligand molecule and consequently metal-complex formation can be understood by the nature and position of absorption bands.

Absorption spectra of polymeric ligands may change drastically by complex formation. The polymer chain adjacent to co-ordinating group influences the absorption band in the spectra.

FTIR has emerged as fast and sensitive technique which is well suited for catalyst studies. FTIR offer number of advantages over disperse IR. The principal advantage of FTIR over IR lies in the much higher signal to noise ratio obtained by FT technique (11a).

Infrared and FTIR spectra of polymer-bound ruthenium and palladium catalysts are given in figs 3.8 to 3.16. Infrared frequencies assignment for the catalysts are

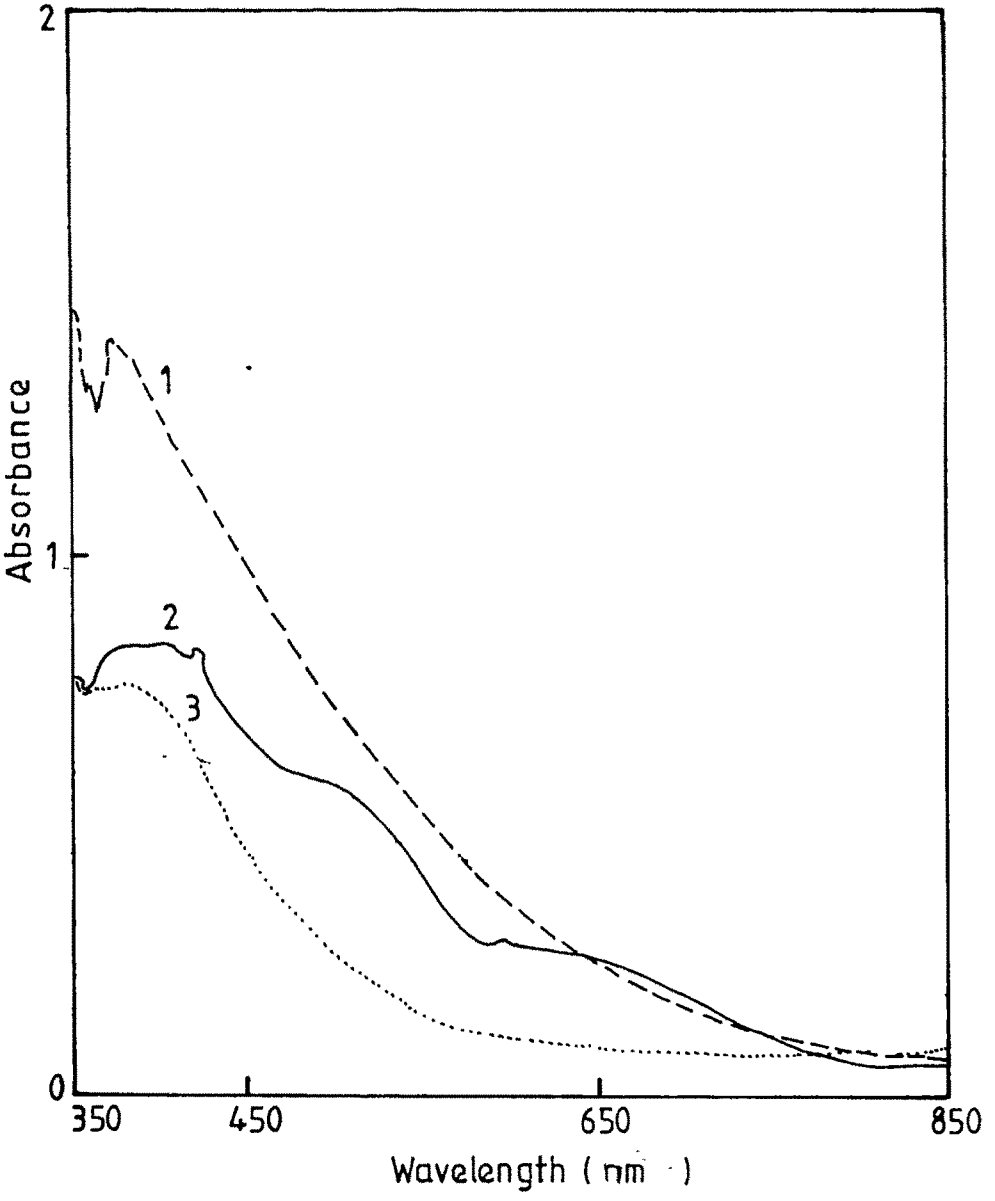

Fig. 3.5 UV-vis relfectance spectra of (1) 2PRu(III)Salen (2) [Pd(II)Salen] (3) 2PPd(II)Salen

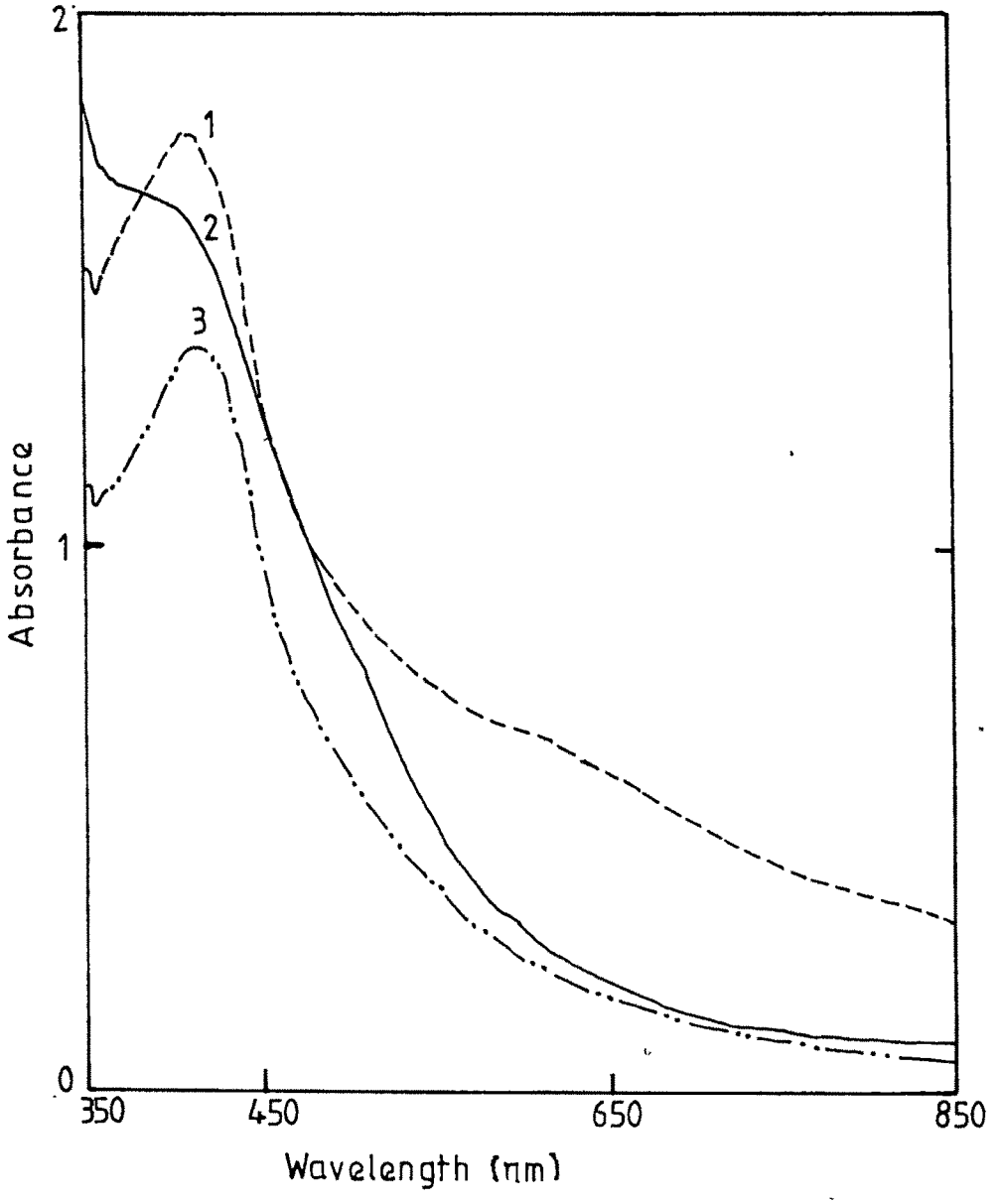

Fig. 3.6 UV-vis reflectance spectra of (1) 8PRu(III)Salen (2) 14PPd(II)Salen (3) 8PPd(II)Salen

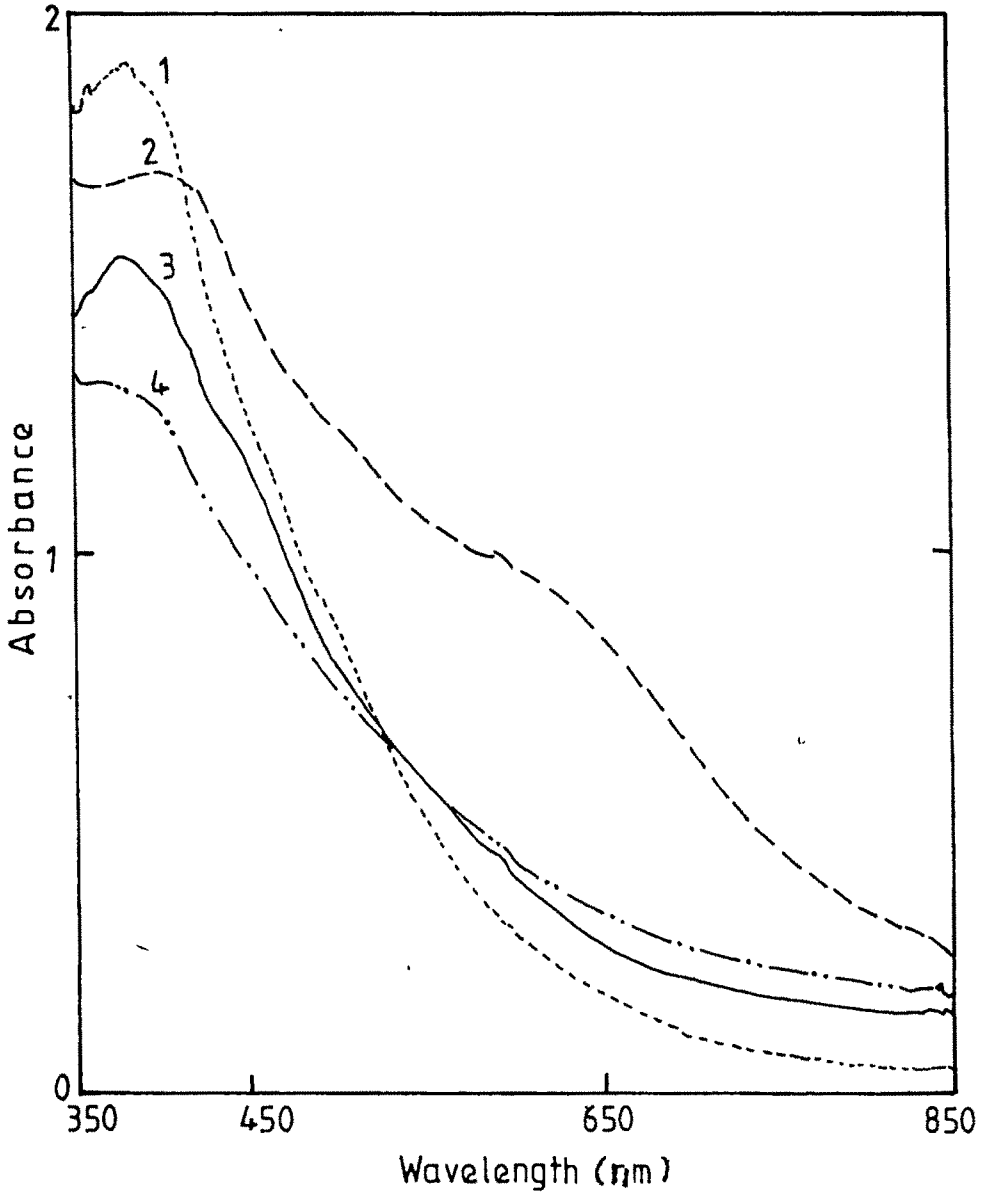

Fig. 3.7 UV-vis reflectance spectra of (1) 8PPd(II)EDTA (2) 14PRu(III)Salen (3) 8PRu(III)EDTA (4) 14PPd(II)EDTA

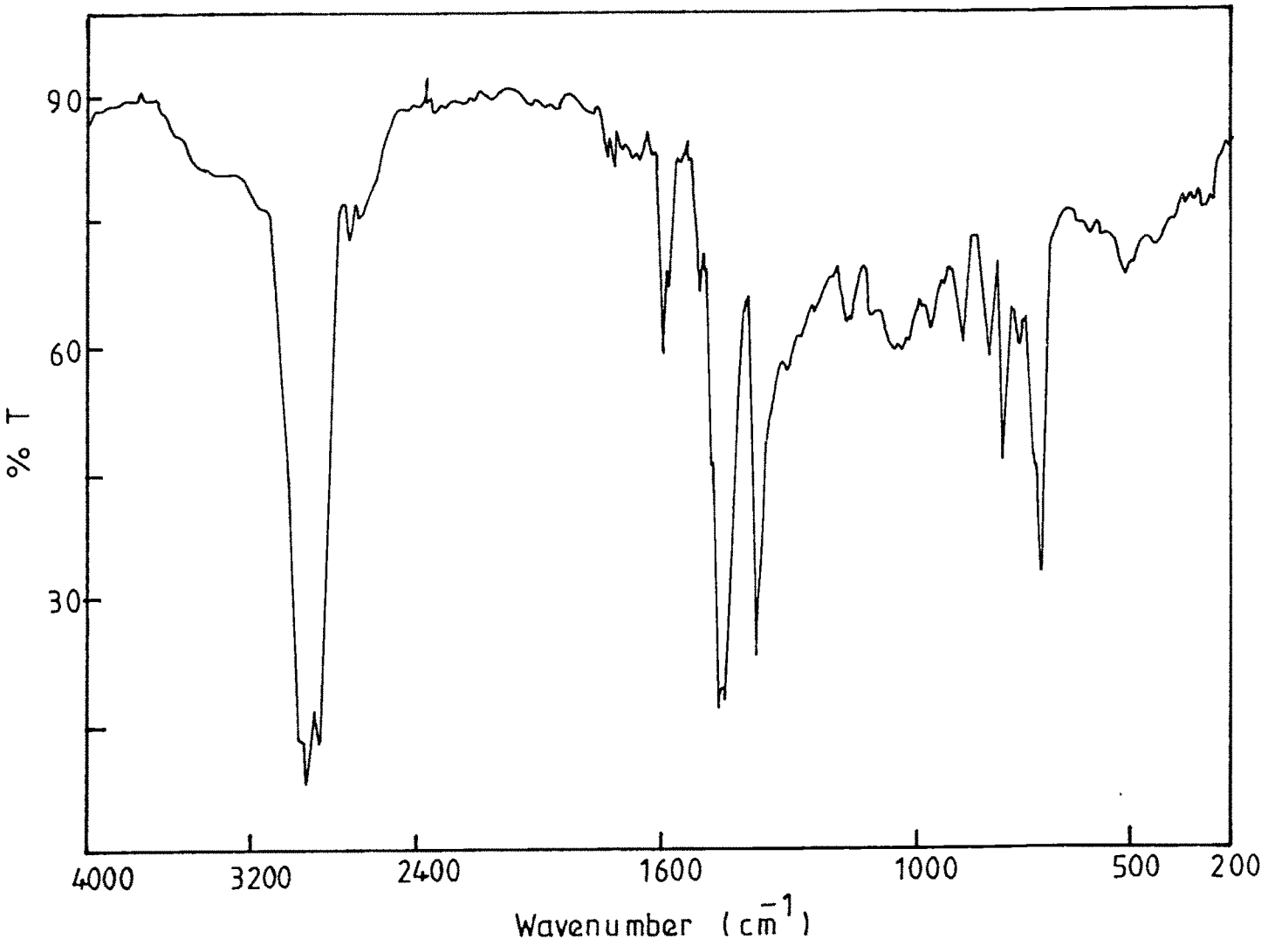

Fig. 3.8 Infrared spectrum of 2PRu(III)Salen

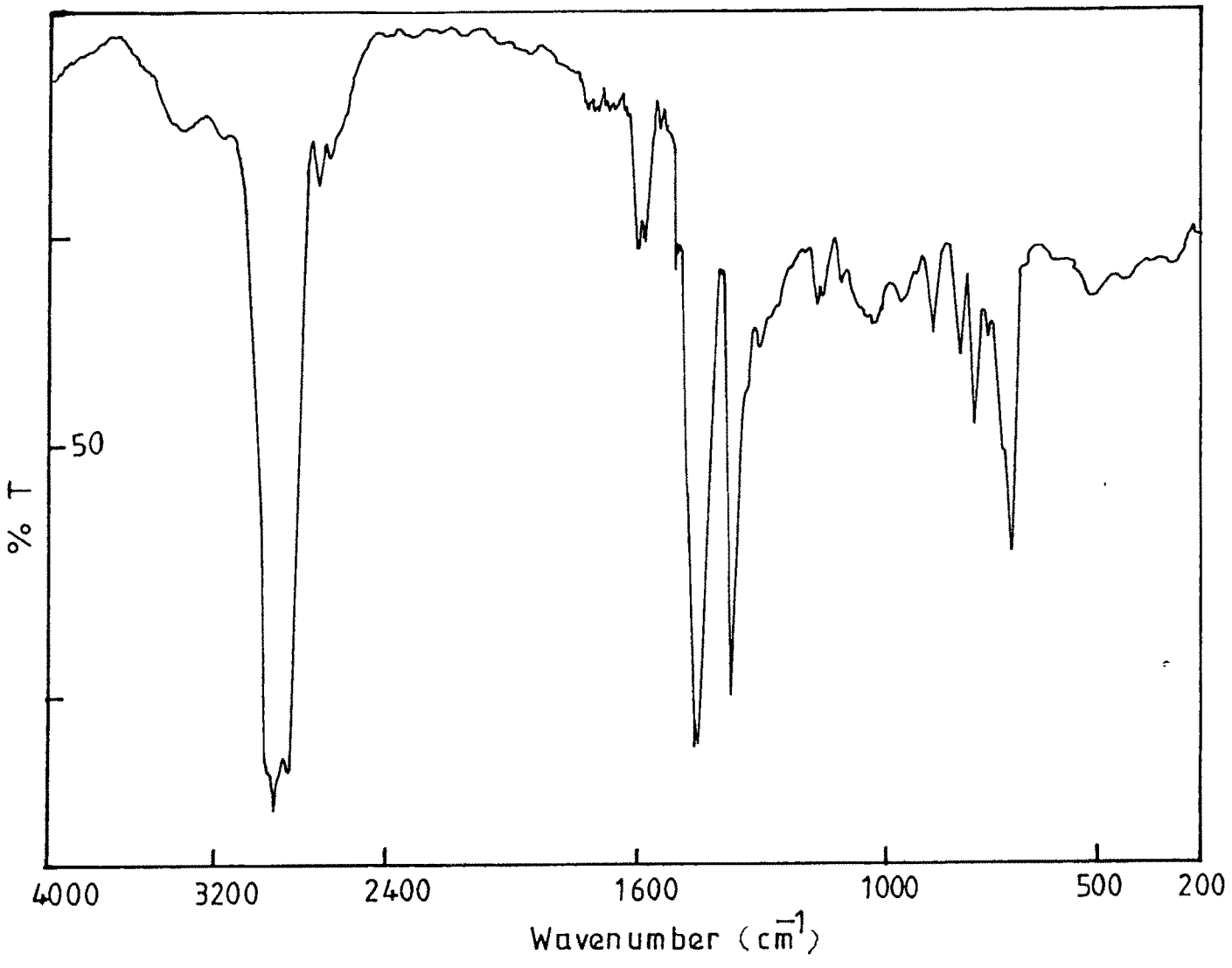

Fig. 3.9 Infrared spectrum of 2PPd(II)Salen

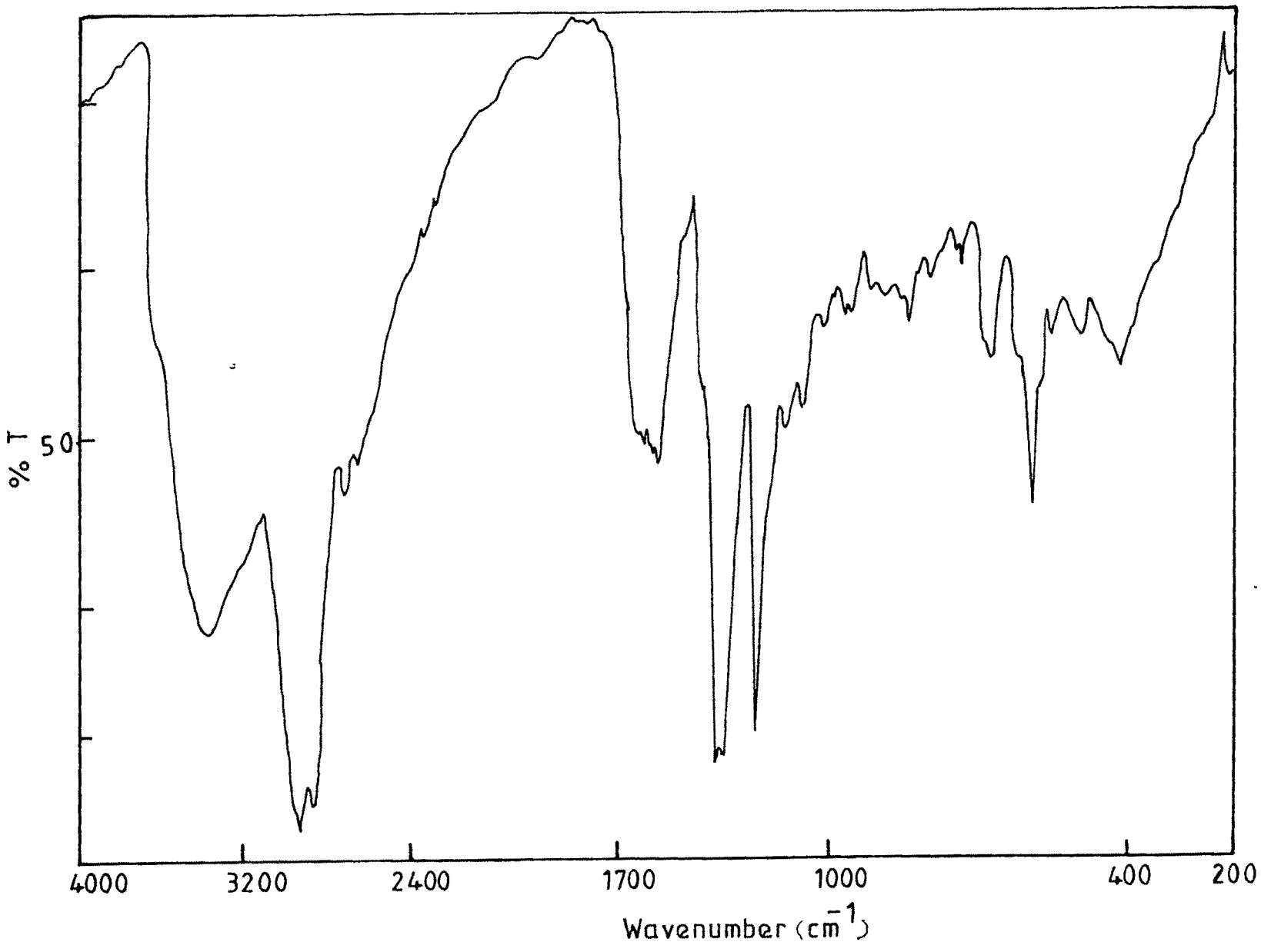

Fig. 3.10 Infrared spectrum of 8PRu(III)Salen

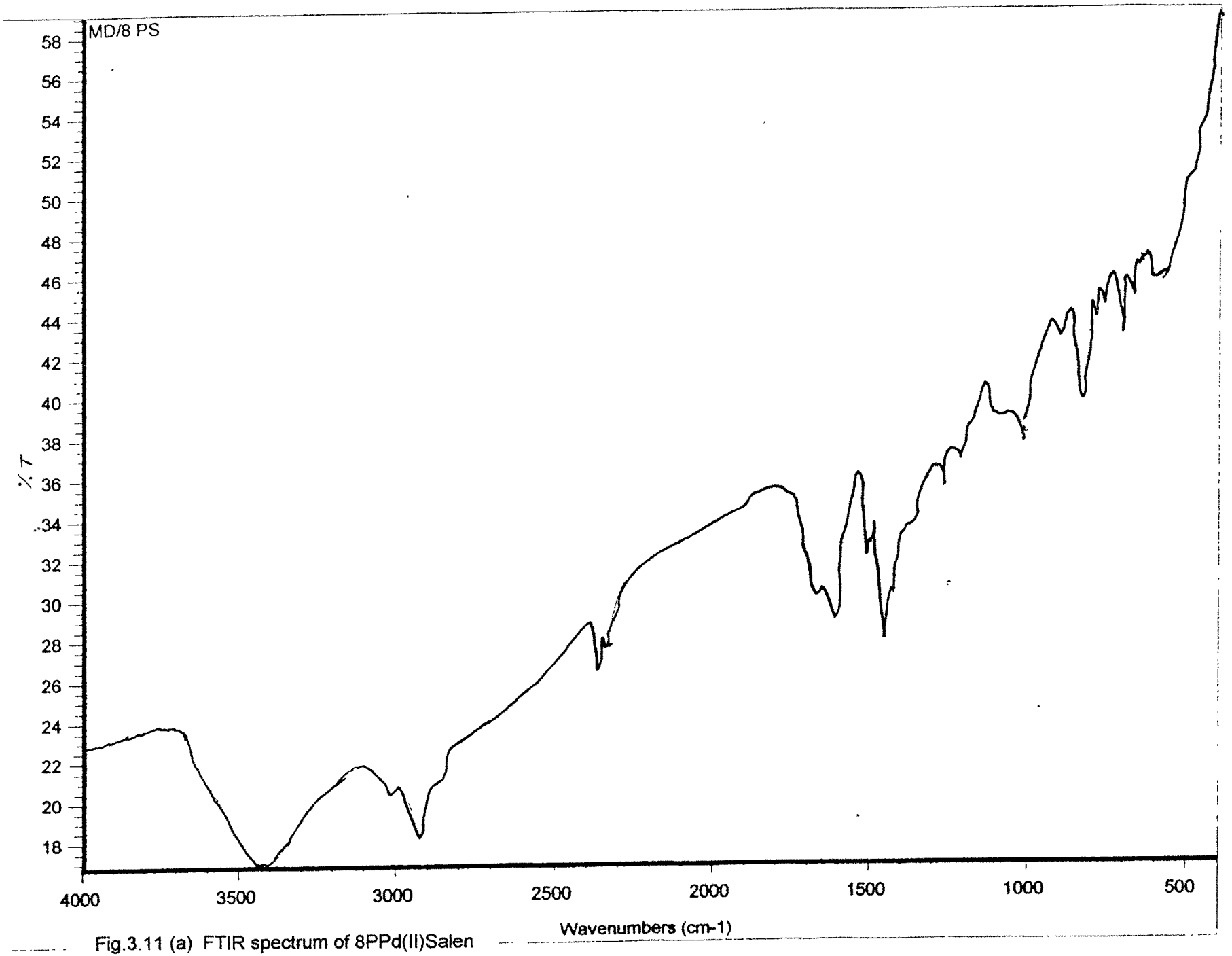

Fig.3.11 (a) FTIR spectrum of 8PPd(II)Salen

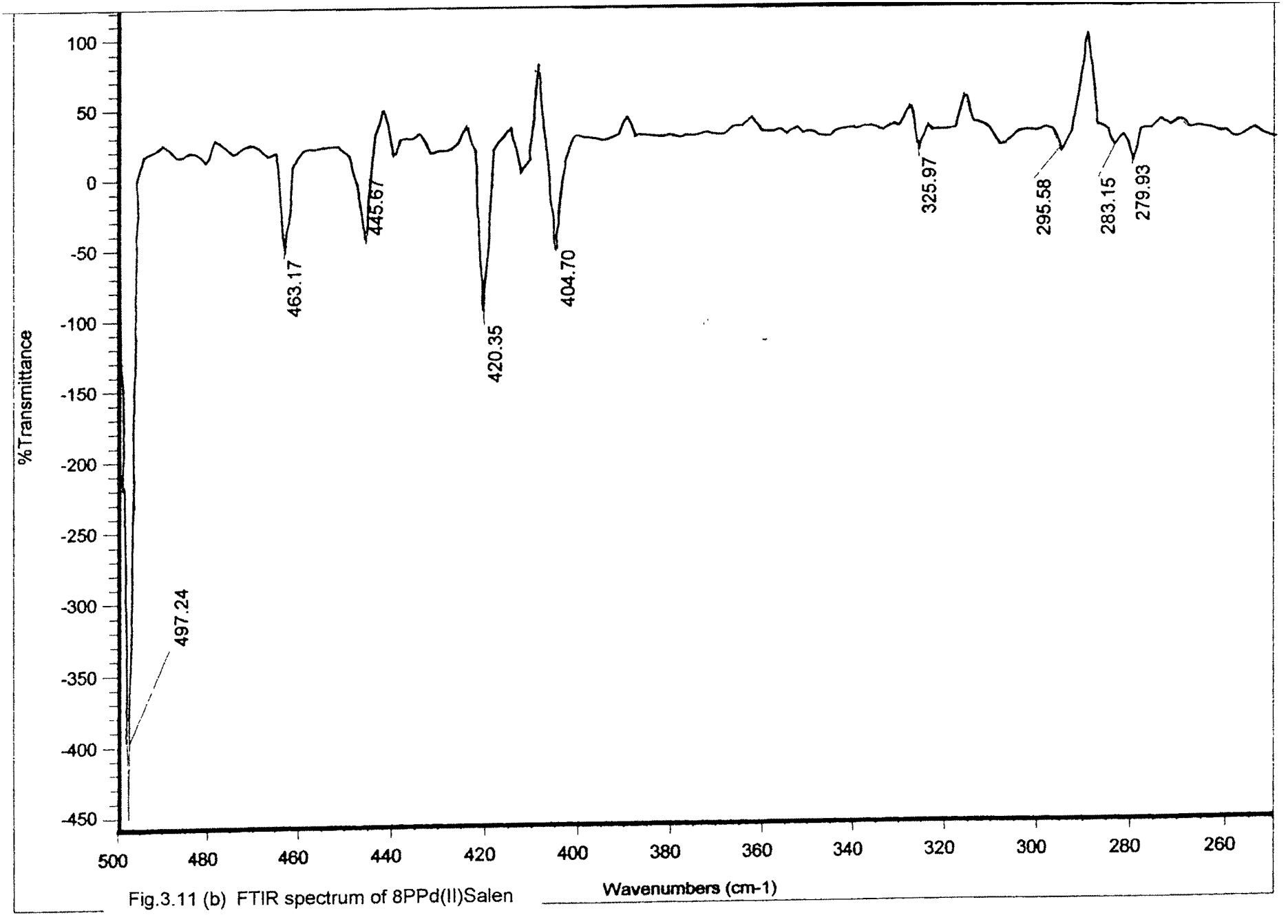

Fig.3.11 (b) FTIR spectrum of 8PPd(II)Salen

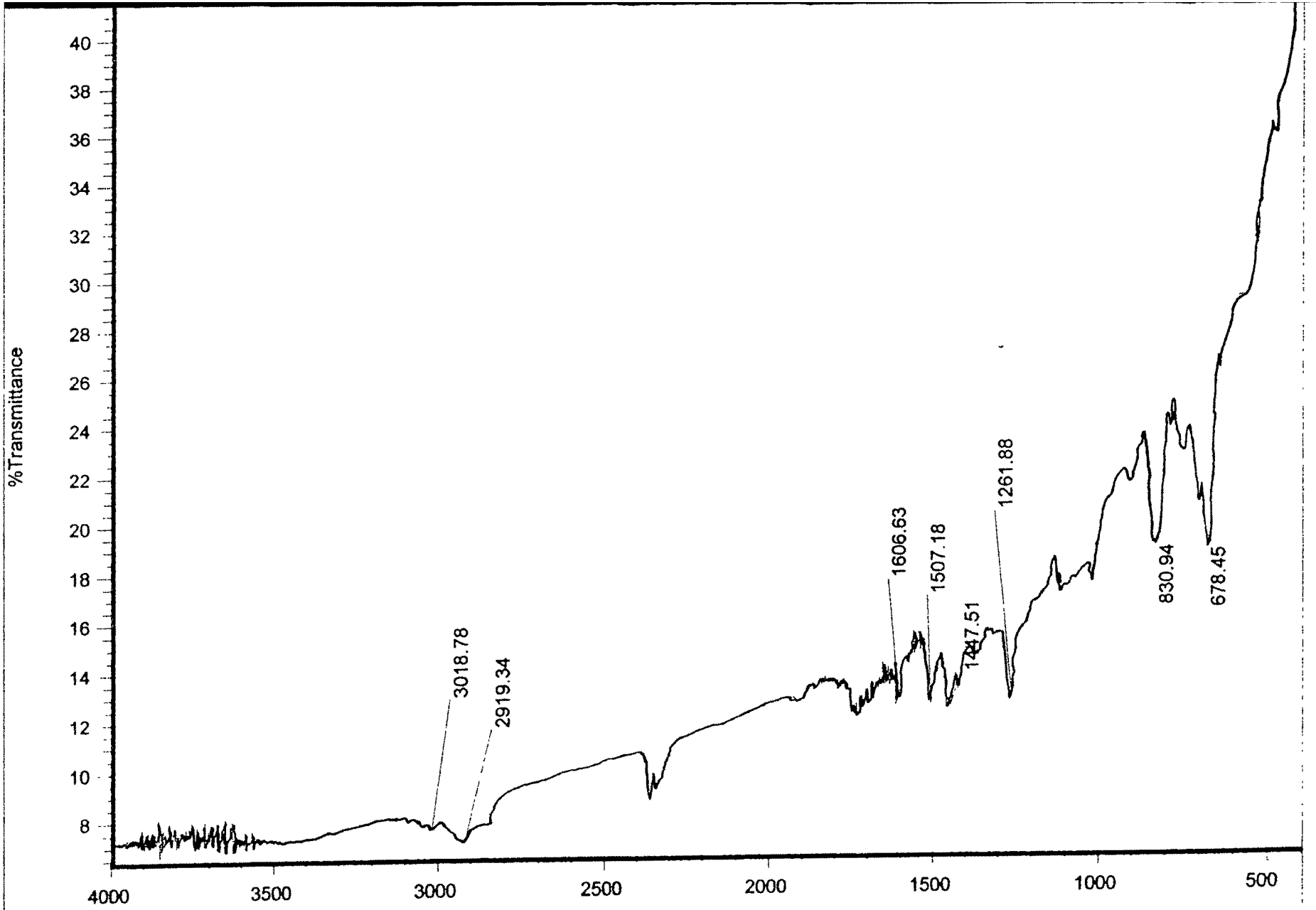

Fig. 3.12(a) FTIR spectrum of 8PRu(III)EDTA

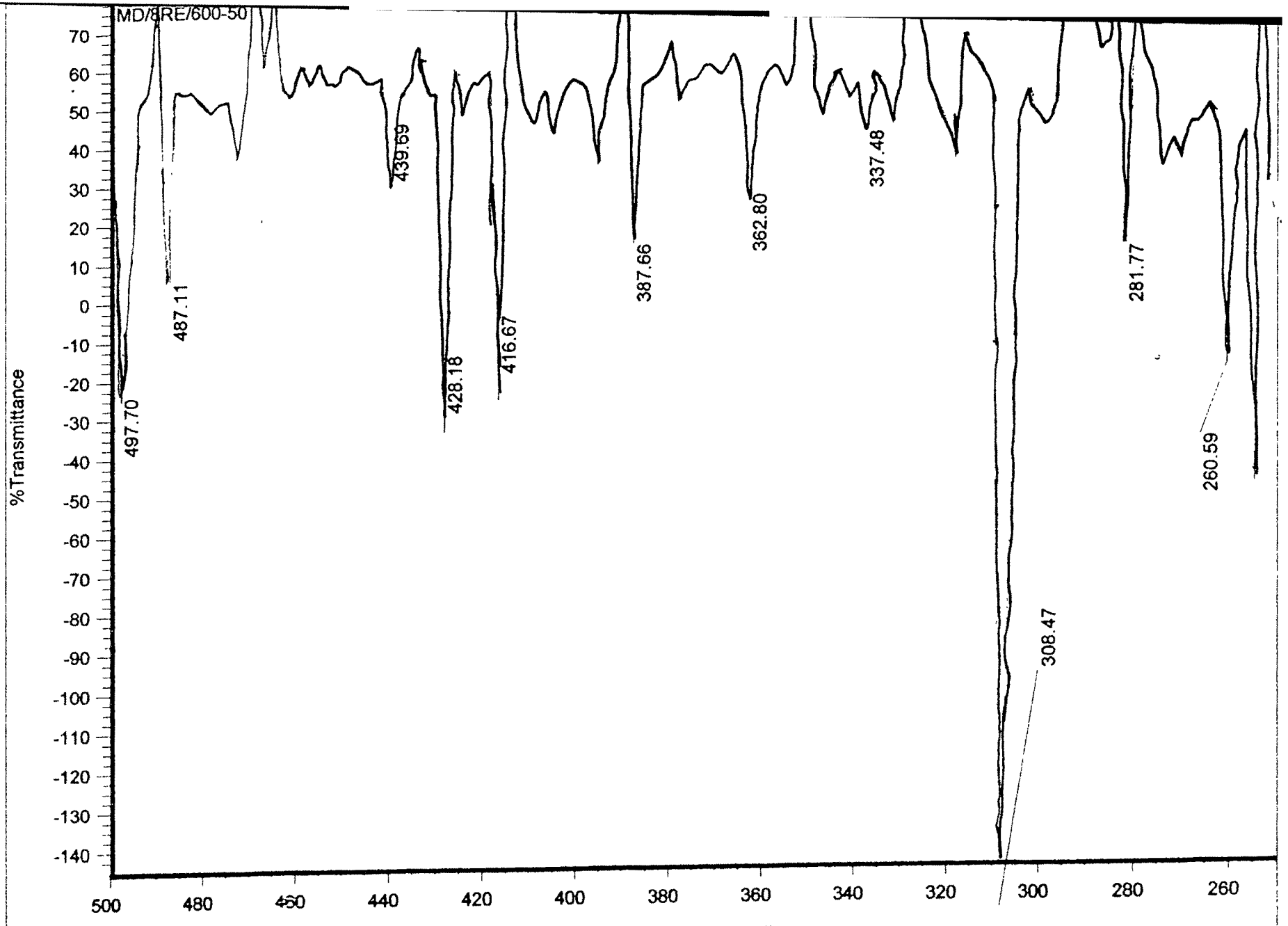

Fig. 3.12(b) FTIR spectrum of 8PRu(III)EDTA

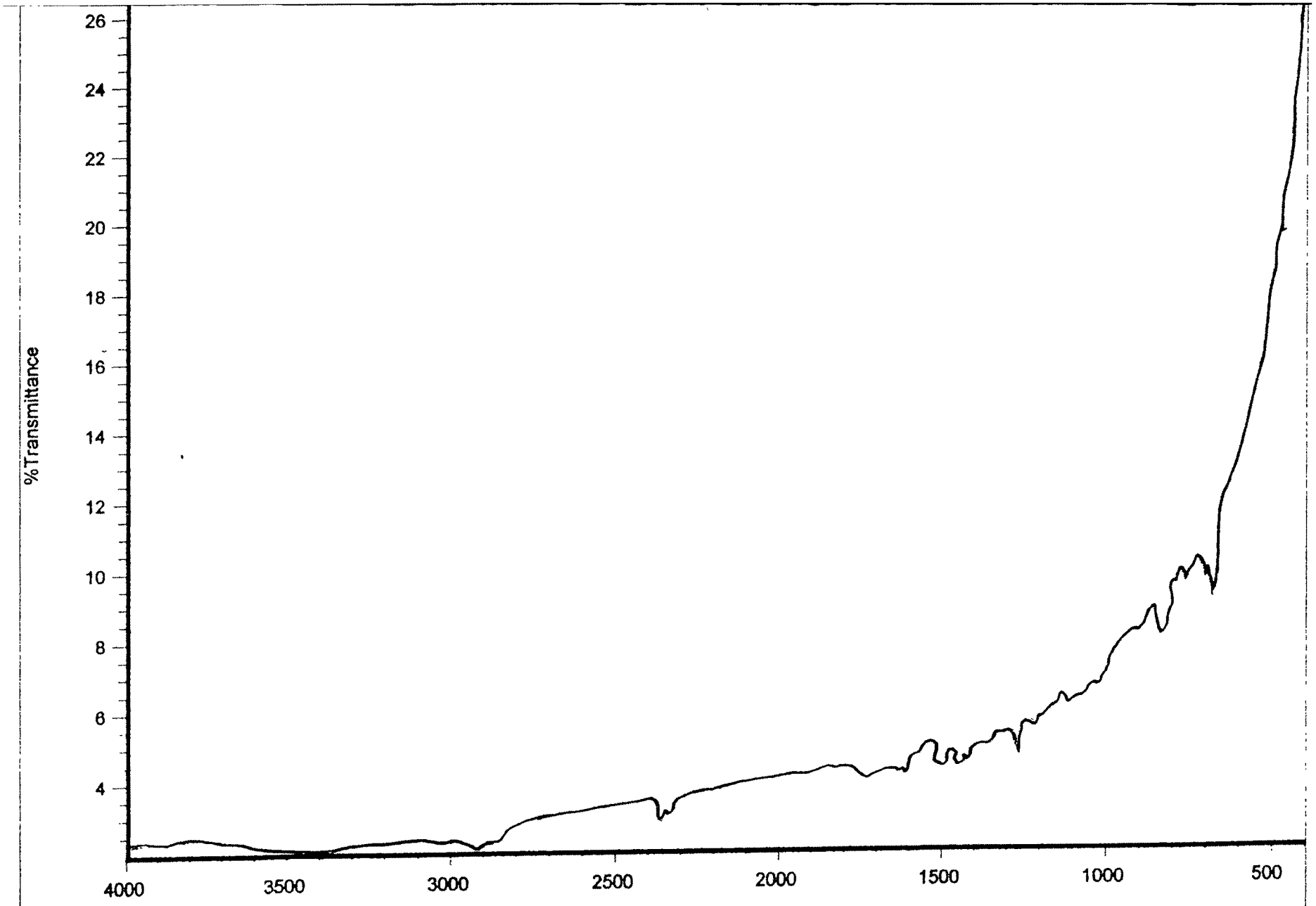

Fig. 3.13(a) FTIR spectrum of 8PPd(II)EDTA

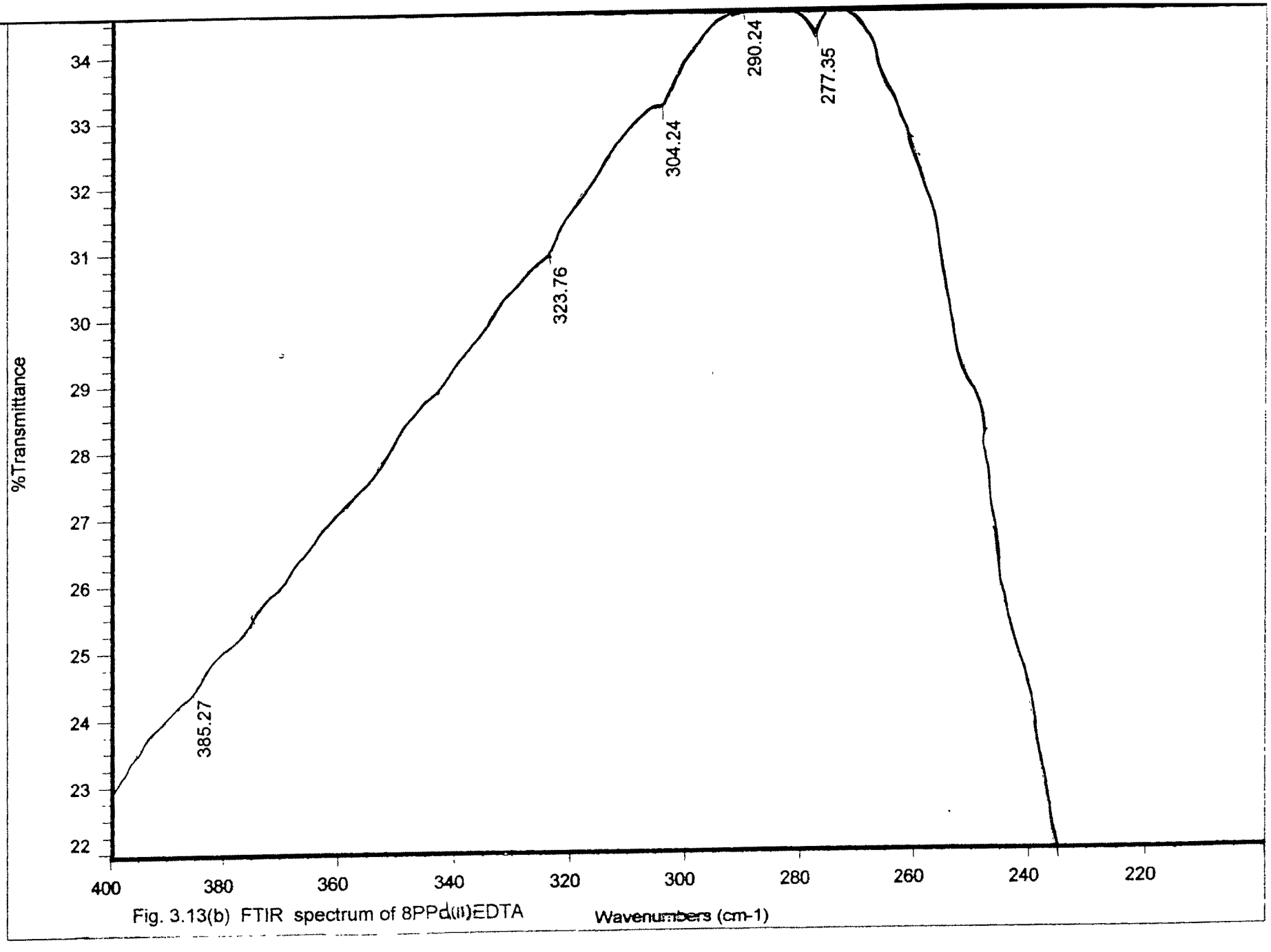

Fig. 3.13(b) FTIR spectrum of 8PPd(II)EDTA

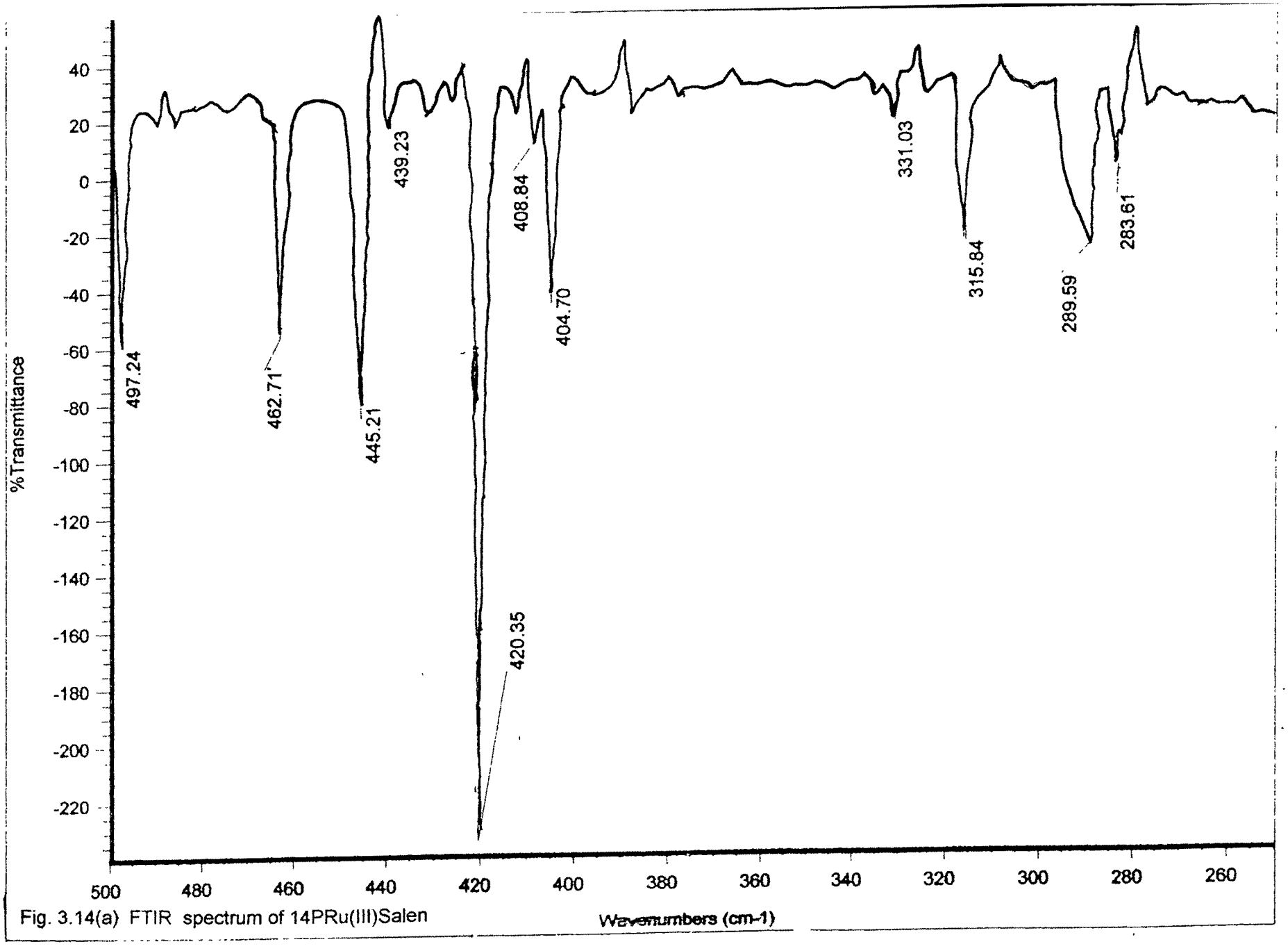

Fig. 3.14(a) FTIR spectrum of 14PRu(III)Salen

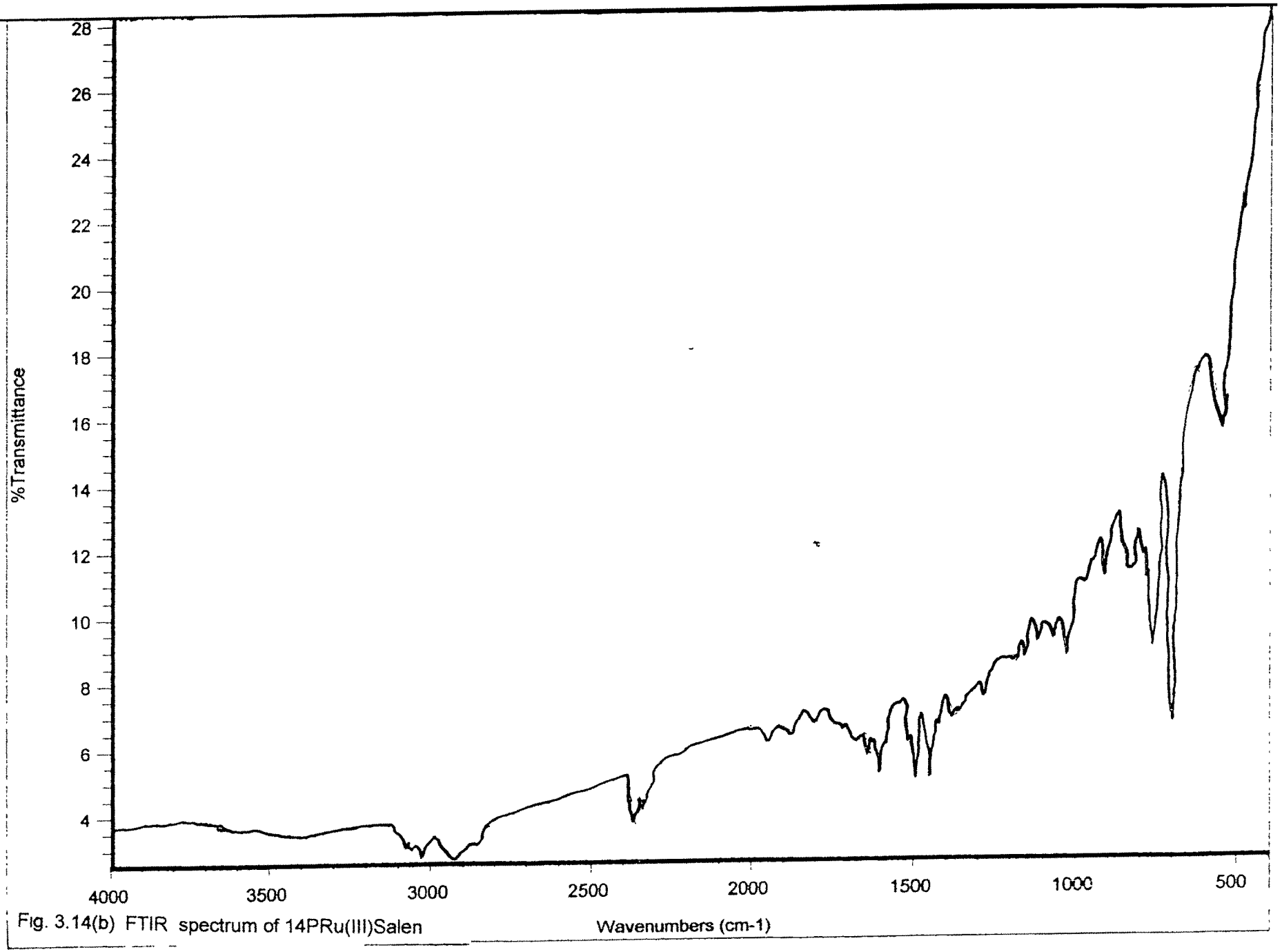

Fig. 3.14(b) FTIR spectrum of 14PRu(III)Salen

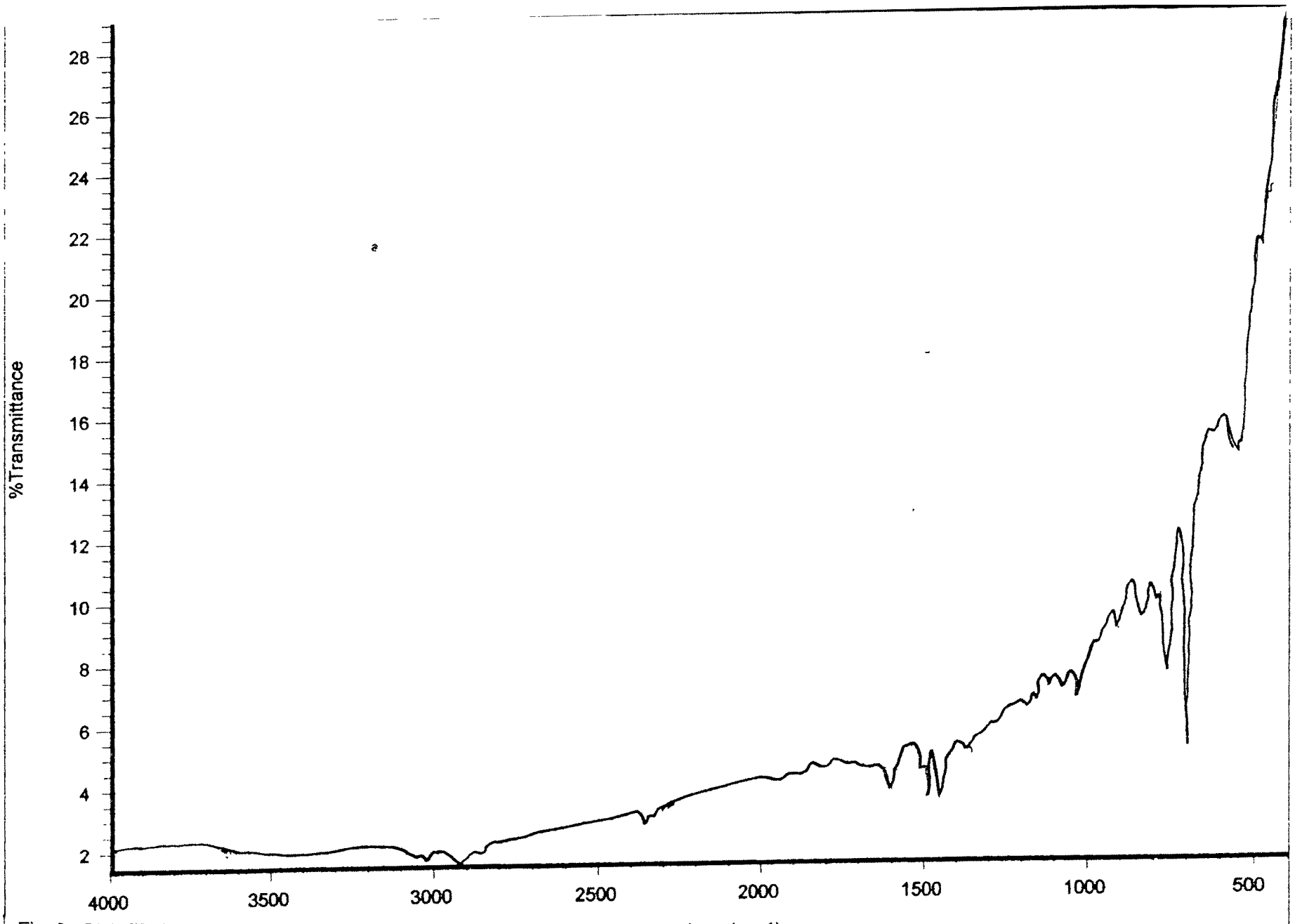

Fig. 3.15(a) FTIR spectrum of 14PPd(II)Salen

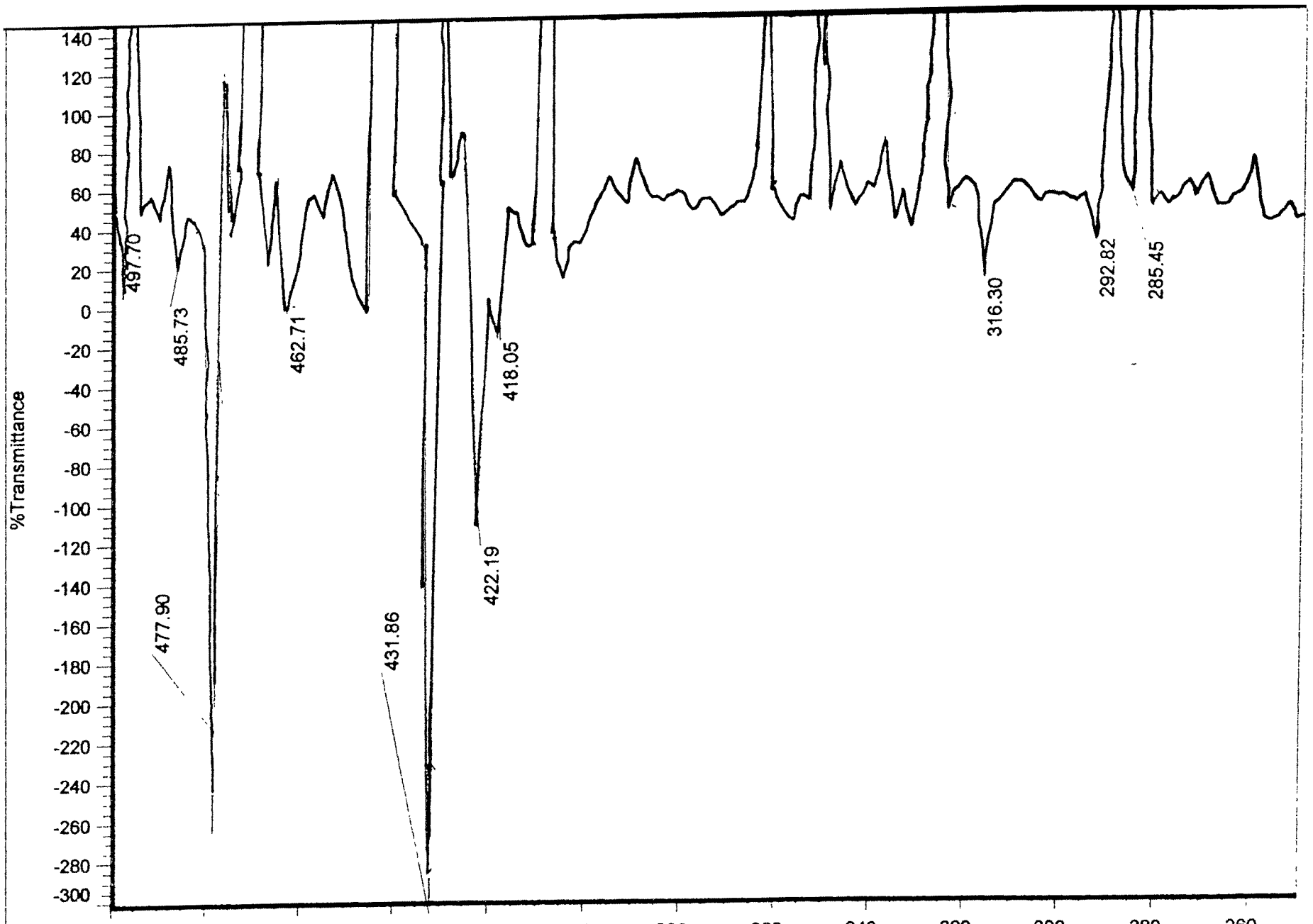

Fig. 3.15(b) FTIR spectrum of 14PPd(II)Salen

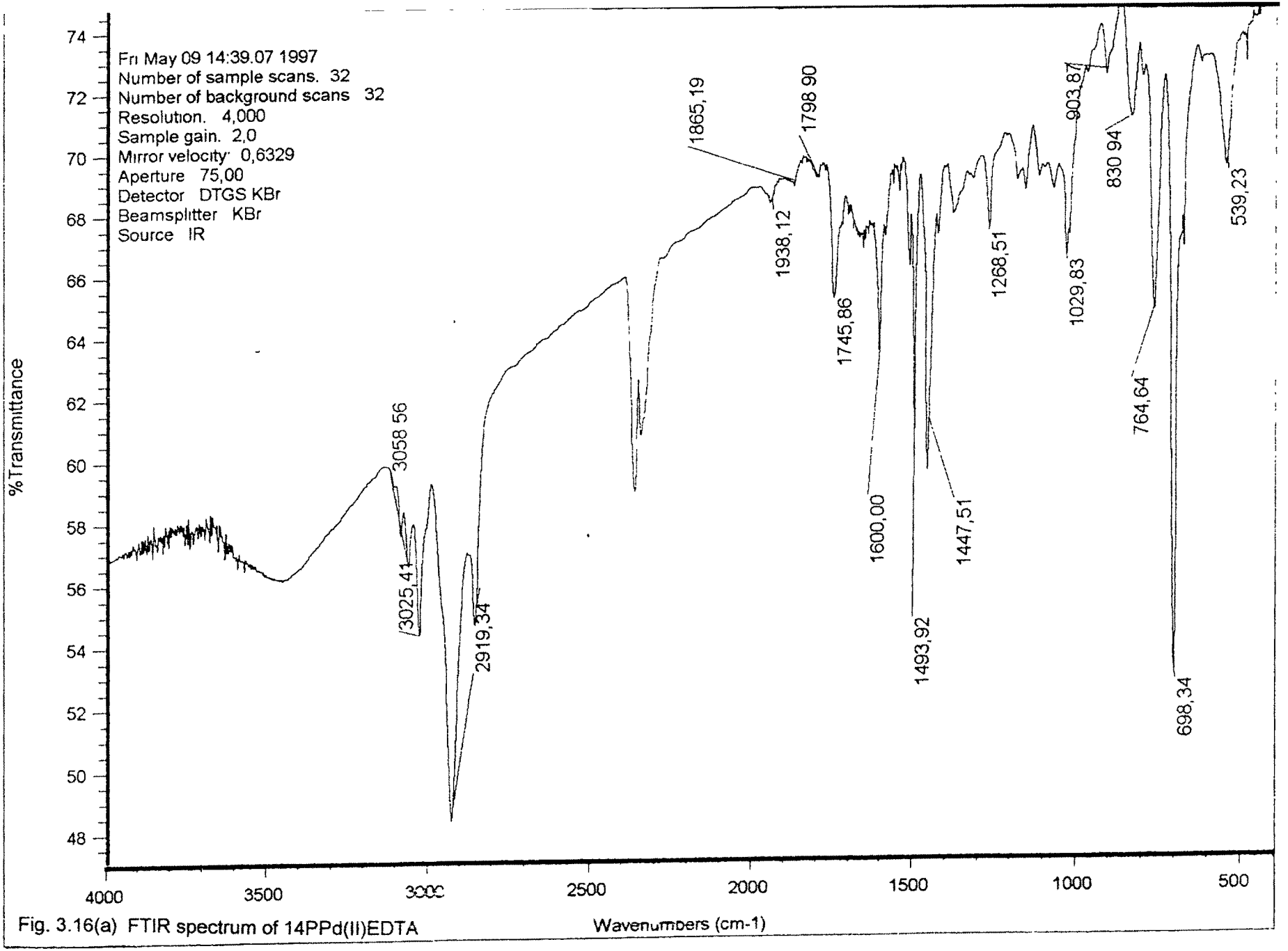

Fig. 3.16(a) FTIR spectrum of 14PPd(II)EDTA

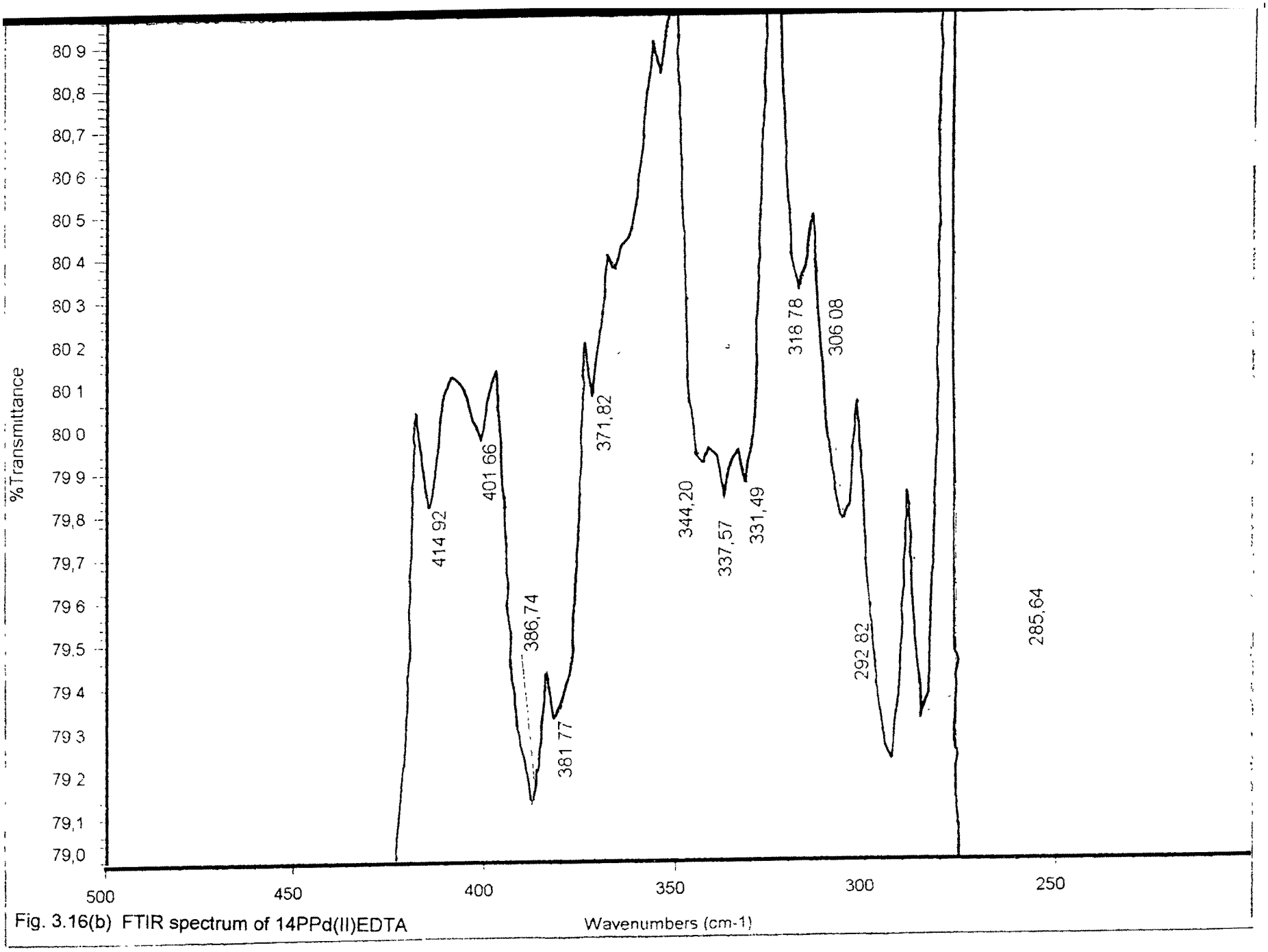

Fig. 3.16(b) FTIR spectrum of 14PPd(II)EDTA

Table 3.8

Summary of the IR frequency assignment for the polymer-bound metal-schiffbase complexes

Catalyst	M-Cl	M-O	M-N	C=N	C-H
2PRu(III)Salen	267	321	440	1604	2924
8PRu(III)Salen	320	513	603	1612	2925
14PRu(III)Salen	283	315	420	1610	2920
2PPd(II)Salen	262	320	440	1604	2922
8PPd(II)Salen	279	420	497	1625	2925
14PPd(II)Salen	292	316	431	1605	2920

M=Ru or Pd

Table 3.9

Summary of the IR frequency assignment for polymer-bound metal-EDTA complexes

Catalyst	M-Cl	M-N	C=0	C-H
8PRu(III)EDTA	260	428	1606	2913
8PPd(II)EDTA	217	567	1738	2855
14PPd(II)EDTA	292	539	1745	2919

M = Ru or Pd

summarised in tables 3.8 and 3.9. Metal-chlorine, metal-nitrogen and metal-oxygen bands are observed.

3.6.3 Electron spectroscopy for chemical analysis (ESCA)

Electron spectroscopy for chemical analysis (ESCA) or x-ray photoelectron spectroscopy (XPS) has been widely used in the characterization of the supported metal complex catalysts since its discovery by Sighbahn and co-workers (12). This technique, based on the famous principle of photoelectron effect invented by Einstein, is currently among most commonly employed physical tools in catalysis research as it provides information about the binding energies of the core electrons. In ESCA, a sample is irradiated by soft x-rays and the electrons knocked out from the various levels in the sample move with velocities depending on the binding energies. Since the binding energy

of the core electron is a fingerprint of the atom, ESCA provides rapid elemental analysis. Due to chemical shift observed in ESCA, chemical state of an atom can also be known

ESCA studies of polymer-bound ruthenium catalysts (fig.3.17 a) gave peaks due to Ru(3p 3/2), Ru(3d 5/2), C(1s), N (1s), Cl(2p 3/2) and O(2s) for Ru-schiff base indicating the presence of Ru in low spin +3 oxidation state. The broadening and shift of ESCA lines may be due to the different chemical environment of polymer-bound Ru complex (13). The ESCA of polymer-bound palladium catalyst (Fig.3.17b) gave peaks due to Pd(3d 3/2), Cl(2p 3/2), N(1s) O(1s) and C(1s) for palladium schiff base, indicating +2 oxidation state of the metal (14).

3.6.4 Electron paramagnetic resonance (EPR)

The electron paramagnetic resonance (EPR), since its discovery by Zaviosky in 1945, has evolved into a very powerful spectroscopic tool for investigating a variety of physico-chemical problems for systems containing paramagnetic species. For conducting EPR investigations, a suitable paramagnetic probe, either intrinsic or extrinsic, would form a part of the system, and this probe should not preferably perturb the environment. This technique finds wide application in the study of solid surfaces and in the identification of surface species (15).

EPR is essential due to transitions between two energy levels of an unpaired electron, corresponding to two spin states in the presence of an external magnetic field. For a free electron, which is not interacting with the surroundings, the transition energy is given by

$$\nu h = \Delta E = g_e H\beta$$

where h = Planck's constant

ν= microwave frequency

B = Bohr magneton

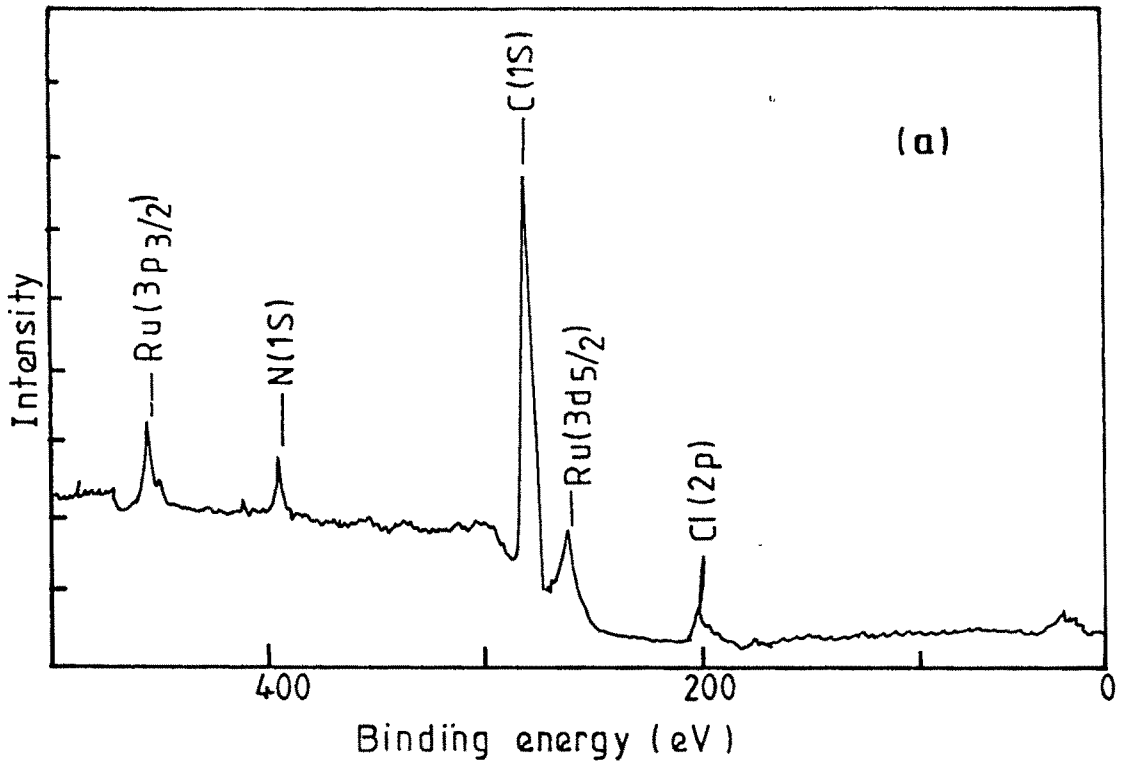

Fig. 3.17(a) ESCA Spectrum of 8PRu(III)Salen
(b) ESCA Spectrum of 8PPd(II)Salen

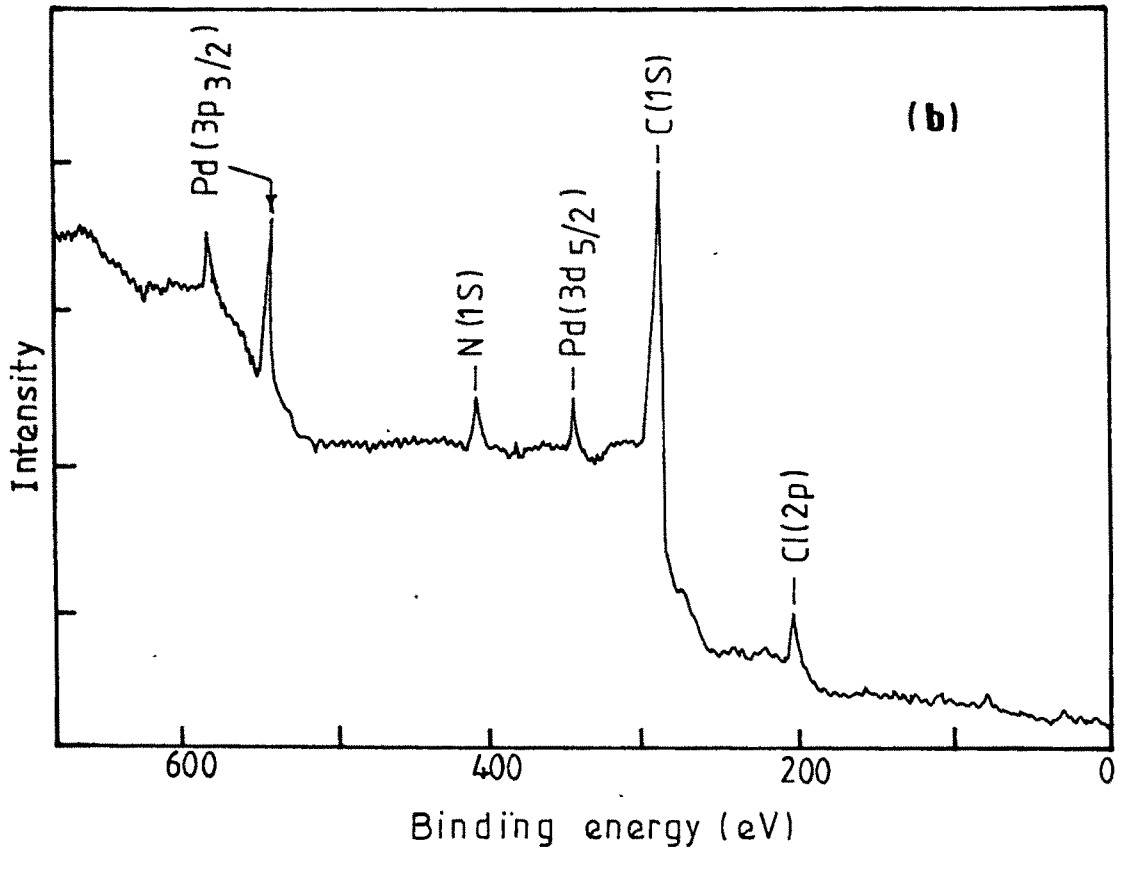

H = strength of external magnetic field

g_e = free electron with g value equal to 2.0023

Thus EPR proves to be an ideal method to probe (i) g factor (ii) identification of paramagnetic species and (iii) for the characterization of environmental symmetry of the ion.

EPR has been used extensively to study the paramagnetic species that exist on various supported catalysts. This technique can only be applied where isolated paramagnetic molecules or ions are present. These should preferably have only one unpaired electron and have neither very short nor very long relaxation times. The technique, therefore has specific, rather than general, applications.

EPR has been used to study Cu(II) on poly-4-vinylpyridine (16), polymer supported chelating amines and schiff bases (17),Ti(IV) on 4-vinylpyridine-divinylbenzene copolymers (18), Ru(III) on polystyrene-divinylbenzene (6) etc.

EPR spectra of catalysts C (8PRu(III)Salen) and H (8PRu(III)EDTA) are given in figs. 3.18 to 3.19. g value for catalyst C was found to be 2.54 (fig.3.18). The $g_{\perp}$ and $g_{\parallel}$ and g_{av} values obtained for the polymer-bound ruthenium complex catalyst H are 2.26, 2.65 and 2.29 respectively (fig. 3.19). This is in agreement with a low spin d^3 centre in a square planer environment, i.e., Ru is present in low-spin +3 oxidation state. Since the spectrum does not resemble a triplet state spectrum, the possibility of Ru being in a +4 oxidation state can be ruled out as low spin Ru(IV) will have two unpaired electrons. The possibility of Ru(II) may also be eliminated because it is diamagnetic and hence EPR inactive. Similar results have been reported by other workers for Ru(III) carbonyl complexes (19). Taquikhan et al have studied the EPR spectra of Ru(III) carbonyl chelates of schiff bases and average g value was obtained to be 2.1, confirming the presence of Ru in +3 oxidation state (20).

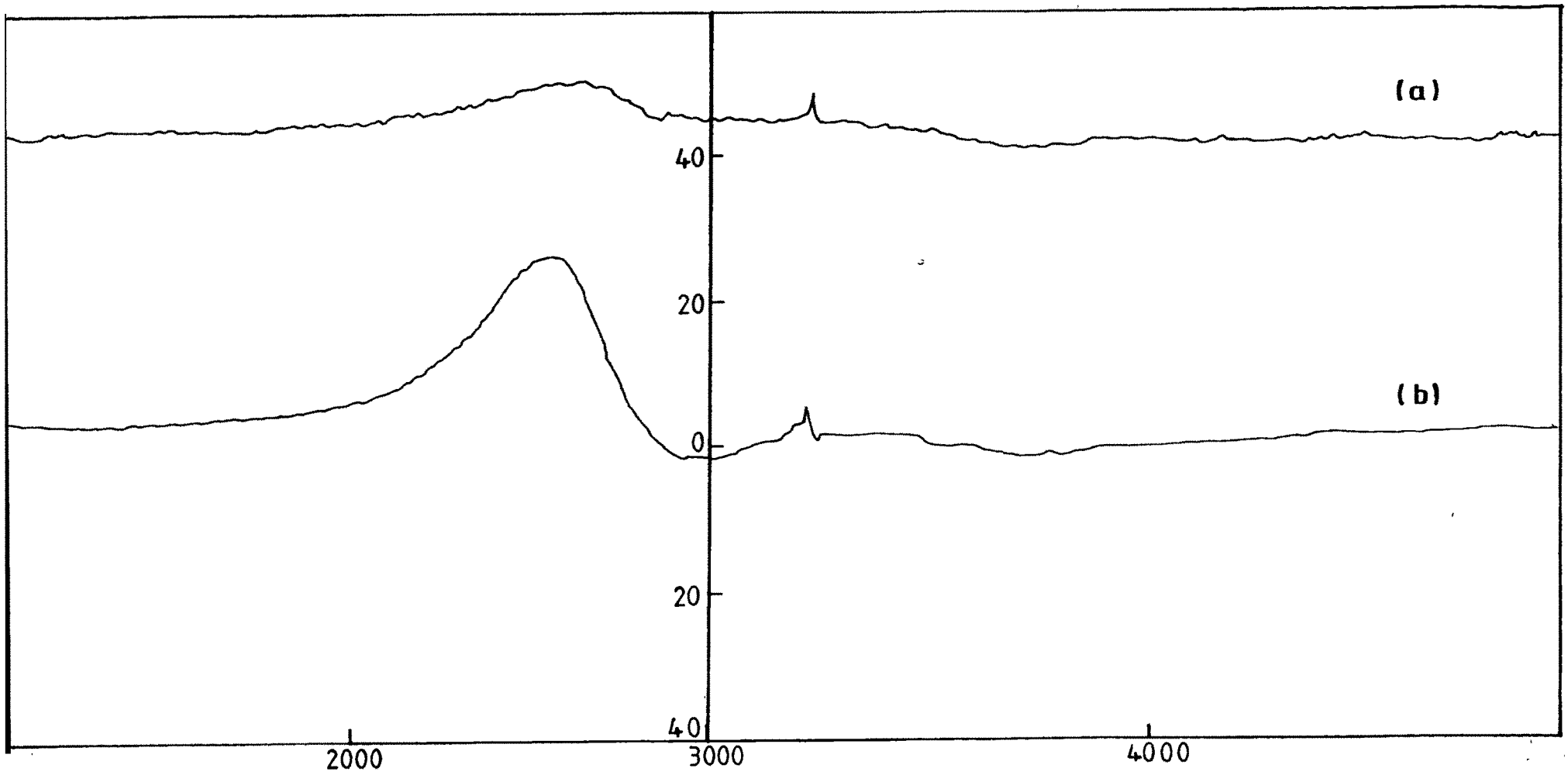

Fig. 3.18 ESR spectra of 8PRu(III)Salen (a) at room temperature (b) at low temperature

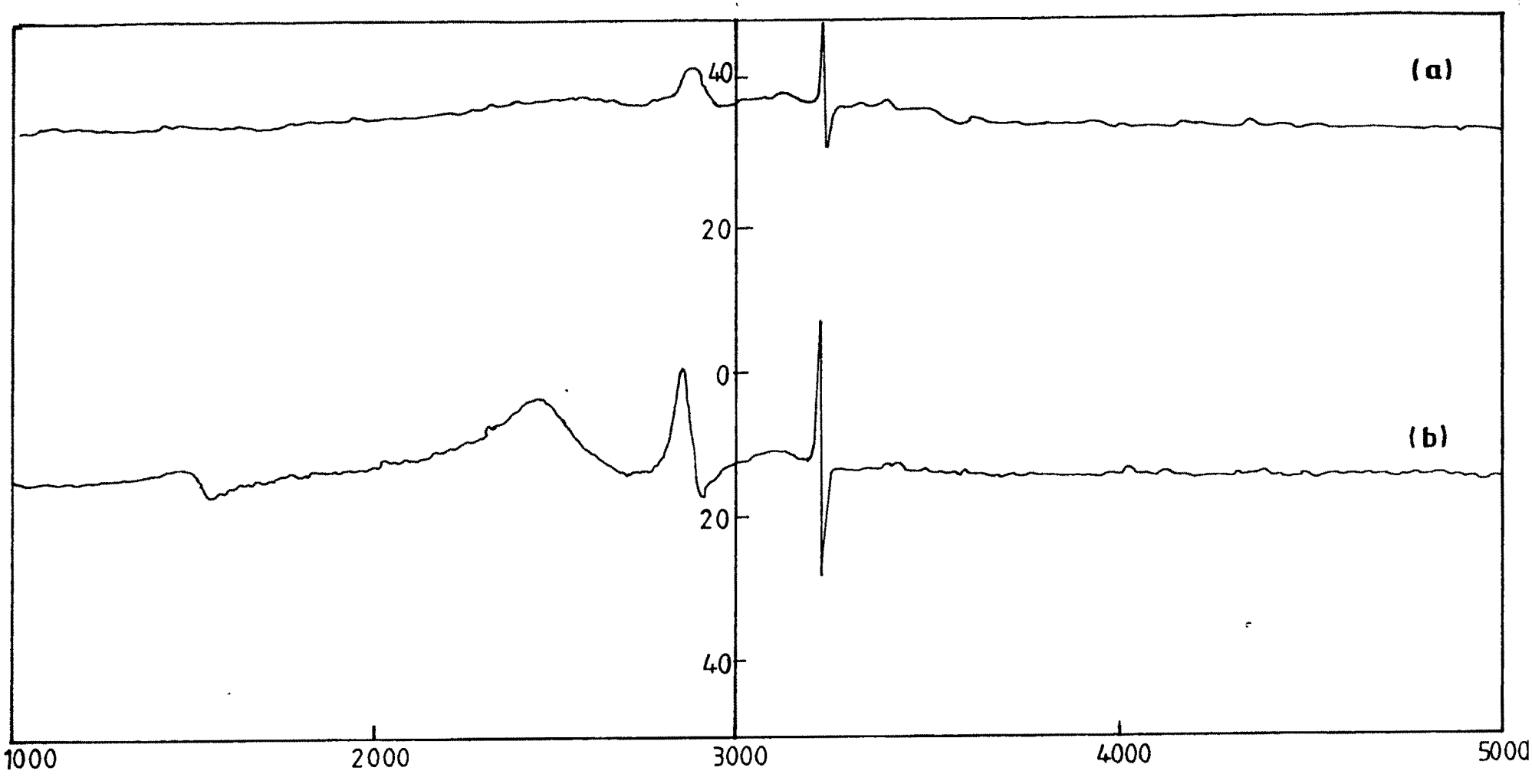

Fig. 3.19 ESR spectra of 8PRu(III)EDTA (a) at room temperature (b) at low temperature

The EPR spectra of unbound complex [Pd(II)Salen] and 8PPd(II)EDTA were found to be inactive. This indicates the diamagnetic nature of Pd(II) ion present in the species. It confirms that Pd is present in +2 oxidation state.

3.7 Morphology of polymer-bound catalysts (SEM)

Scanning electron microscopy (SEM), used for imaging topography of a solid surface, is based on the analysis of the yield of secondary electrons (coming mostly from the sample surface) or back-scattered electrons (which arise from within the sample, where scattering by heavier atoms is more important) as a function of the location of the primary beam with respect to the sample. The contrast arises from the orientation of the surface with respect to the detector.

The catalytic behaviour depends upon the structure and composition of active component as well as morphology of its supporting medium. Morphology of polymer-bound catalysts can be observed at a range of magnification (few hundred to few million times) which provide information about the nature of porosity, the nature and the distribution of the active components, etc. Comparison of porosity of different supports is also possible.

The morphology of polymer supports and catalysts was studied using SEM. Micrographs are given in Plates 3.1 and 3.3. It was observed that the beads are porous and the texture changes with the change in degree of cross-linking. A change in the shape of polymer beads has been observed after anchoring the metal complexes.

3.8 Thermal stability

Thermal stability of a catalyst has a direct consequence/impact on its applicability. The change in weight and thermal property of a catalyst with changing experimental conditions can be used for a variety of studies. In case of polymer-bound metal complex catalysts weight loss or heat change may reveal the stability and phase change as a

Plate 3.1 Scanning Electron Micrographs of
(a) XAD-2 (b) 2PRu(II)Salen (c) 2PPd(II)Salen
(d) 8% cross-linked P(S-DVB)

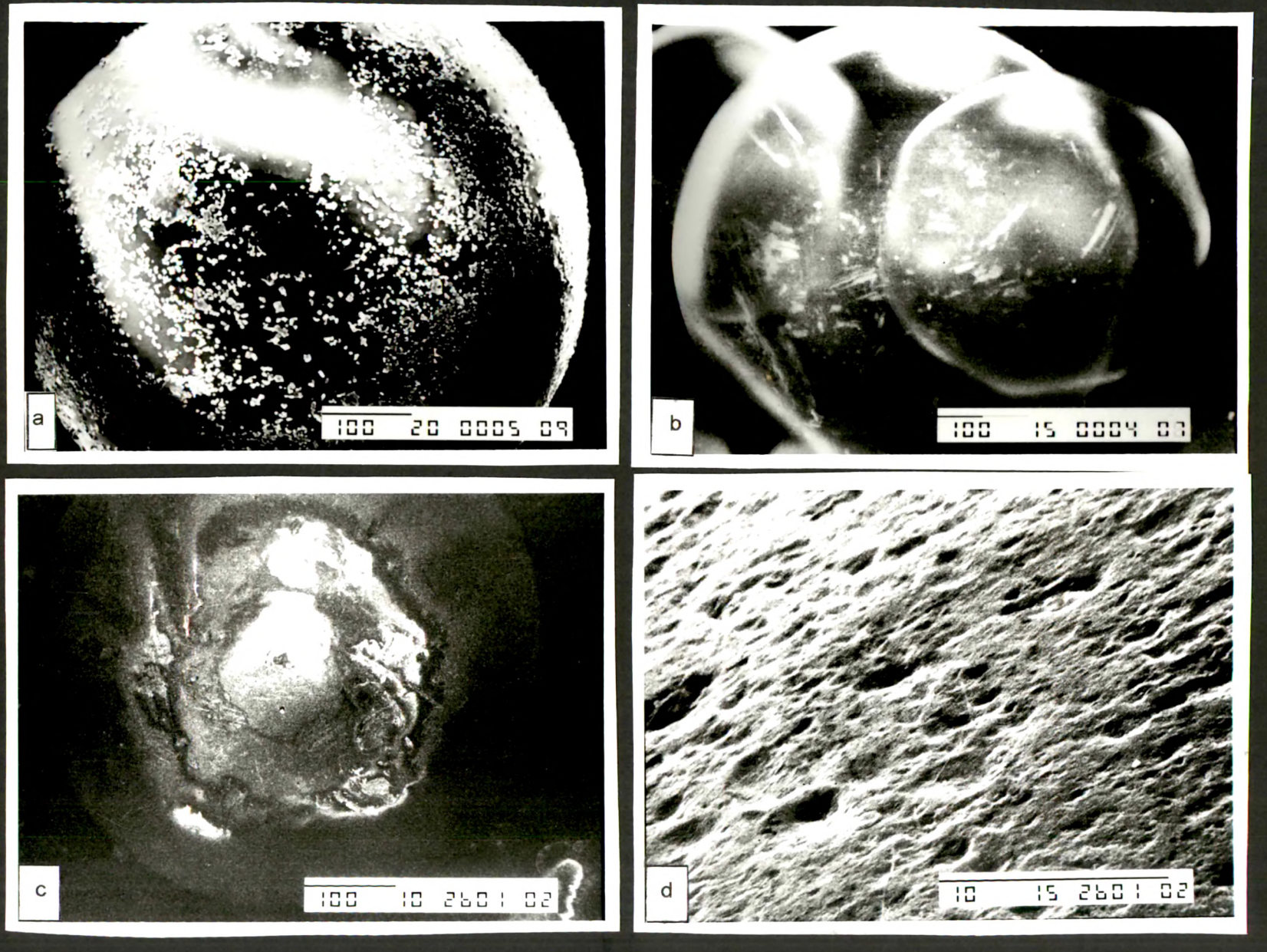
a
100 20 0005 09
b
100 15 0004 07
c
100 10 2601 02
d
10 15 2601 02

Plate 3.2 Scanning Electron Micrographs of
(e) 8PRu(III)Salen (f) 8PPd(II)Salen
(g) 8PRu(III)EDTA (h) 8PPd(II)EDTA

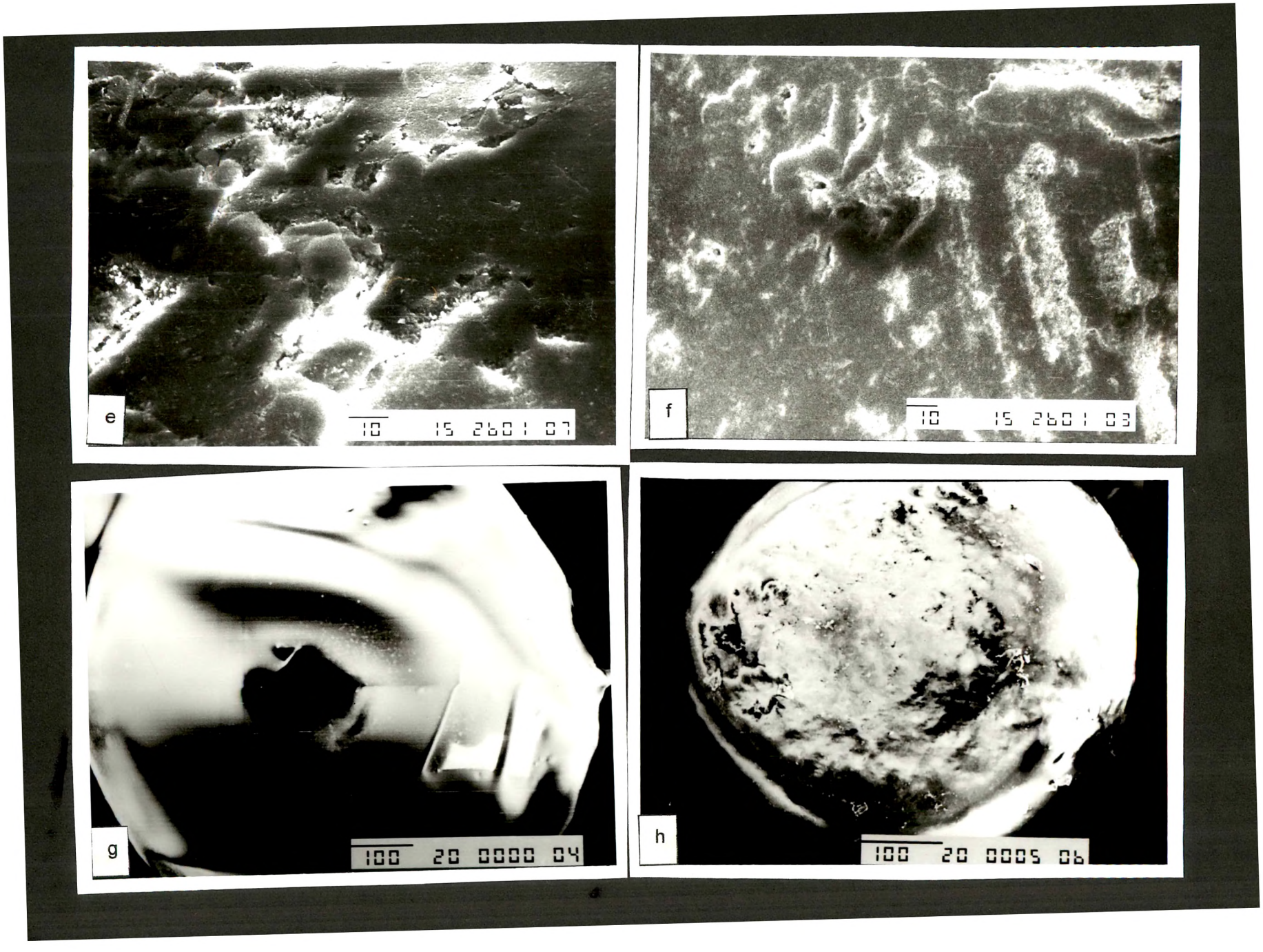
e
10 15 2601 07
f
10 15 2601 03
g
100 20 0000 04
h
100 20 0005 06

Plate 3.3 Scanning Electron Micrographs of
(i) 14% cross-linked P(S-DVB) (j) 14PRu(III)Salen
(k) 14PPd(II)Salen (l) 14PPd(II)EDTA

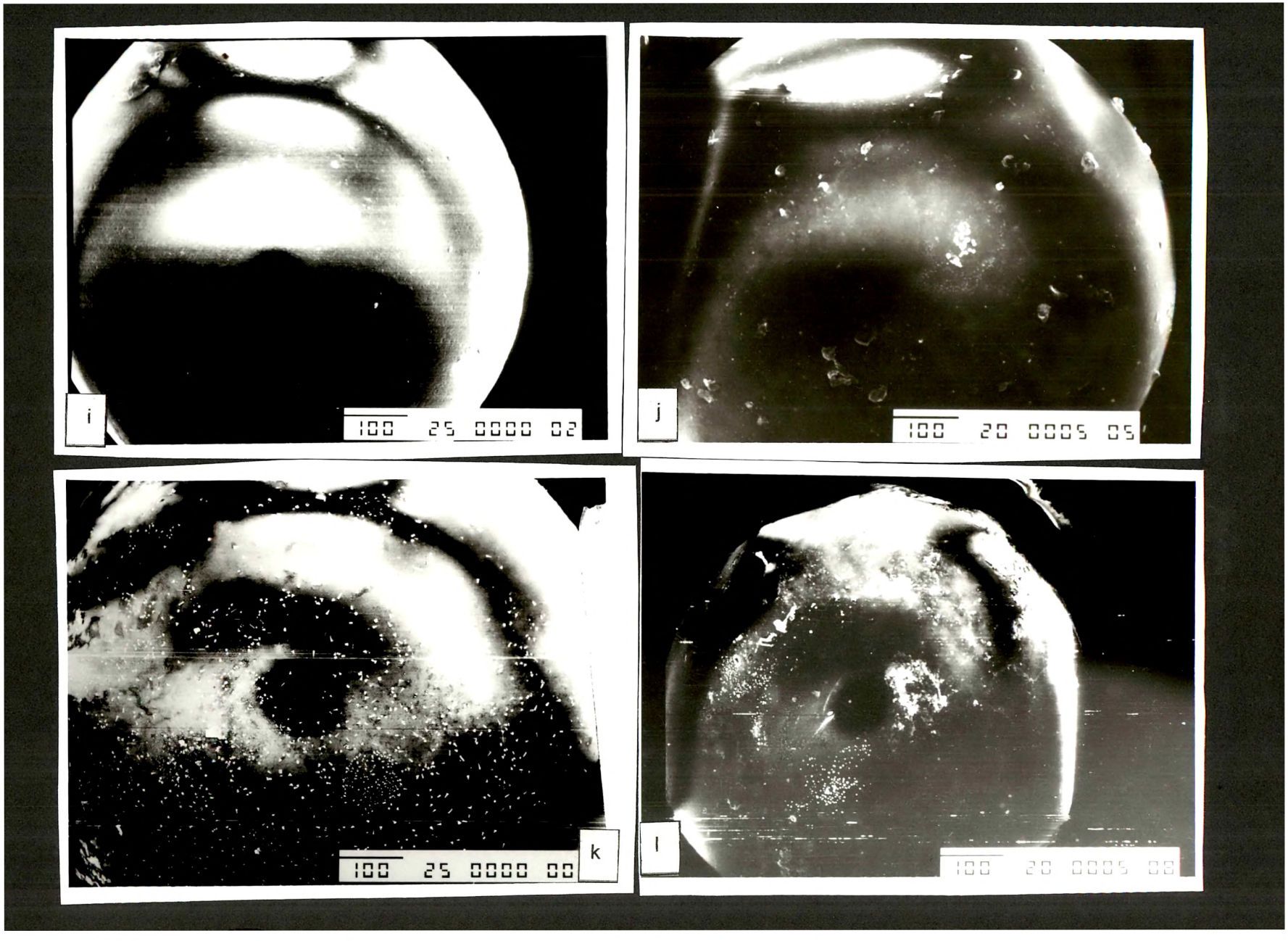
i
100 25 0000 02
j
100 20 0005 05
k
100 25 0000 00
l
100 20 0005 08

function of environment.

Thermal stability of homogeneous metal complexes is reported to be enhanced when supported on organic polymers or inorganic oxides (21). Thermal property of the polymer support vary with the cross-linking of the polymer. Thus determination of thermal behaviour of polymer-supports and polymer-bound catalysts needs investigation in order to know about the limit of catalytic reaction temperature.

Fig. 3.20 shows thermogravimetric analysis (TGA) of styrene-divinylbenzene copolymers of different cross-linking used as polymer supports. 2% and 8% cross-linked polymer supports are less stable than 14% cross-linked support. Hydrophobic polymer supports XAD-2 and AM-44 are stable upto 150°C and the degradation starts above 200°C. Initial weight loss found is due to moisture content. AM-24 (14% cross-linked) polymer support was found to be stable upto 350°C. Thus, it could be concluded that XAD-2 and AM-44 can be used safely upto 100°C whereas AM-24 can be used safely upto 350°C. Thus thermal stability of the polymer was found to increase with increase in cross-linking.

Figs. 3.21 to 3.22 show TGA curves for the polymer-bound catalysts. Change in the thermal stability of catalysts after supporting the metal ions on to the polymer surface is observed.

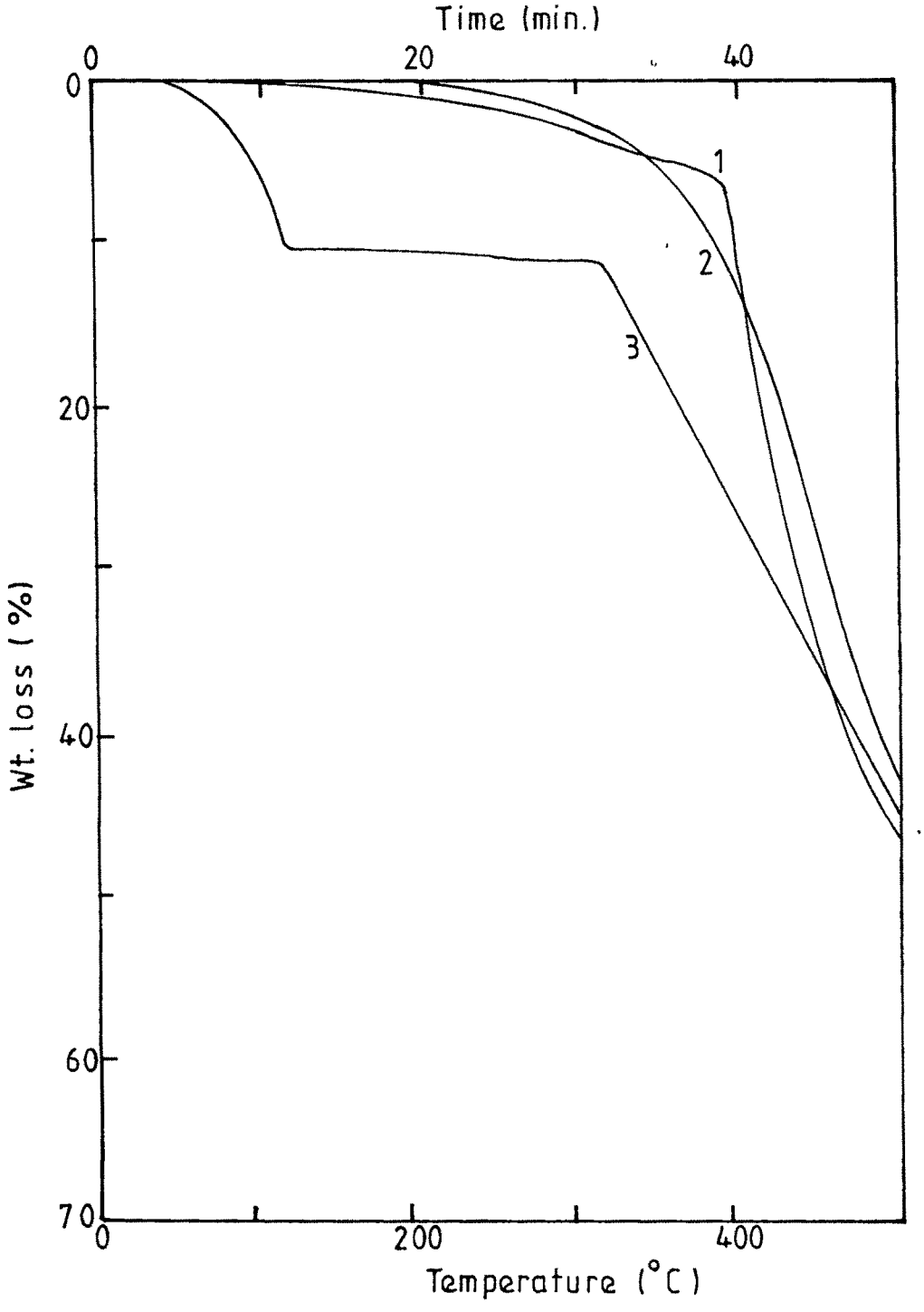

Fig. 3.20 Thermogravimetric curves of (1) 2PRu(III)Salen (2) 2PPd(II)Salen (3) XAD-2

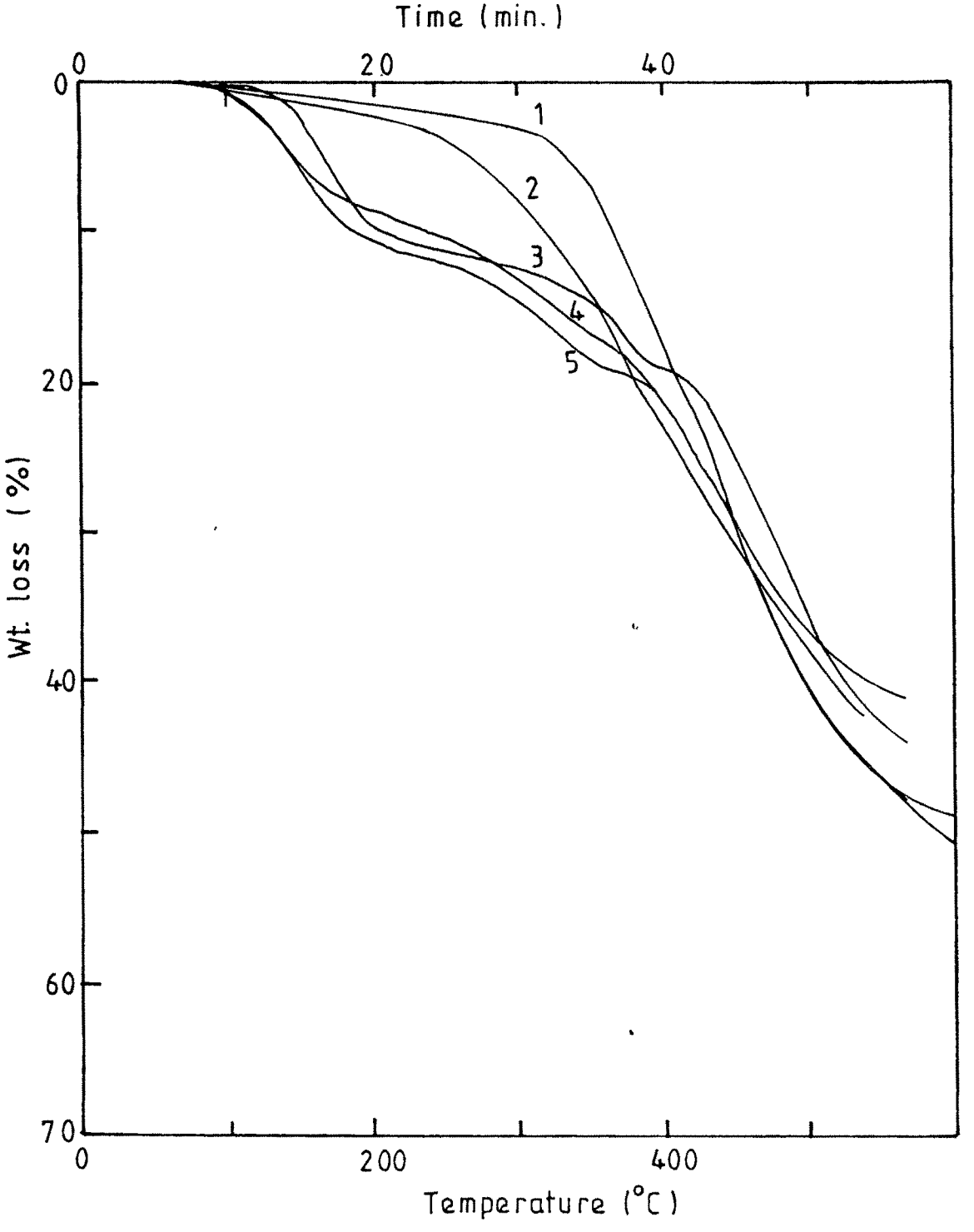

Fig. 3.21 Thermogravimetric curves of (1) 8PRu(III)EDTA (2) 8PPd(II)EDTA (3) P(S-DVB) 8% cross-linked (4) 8PPd(II)Salen (5) 8PRu(III)Salen

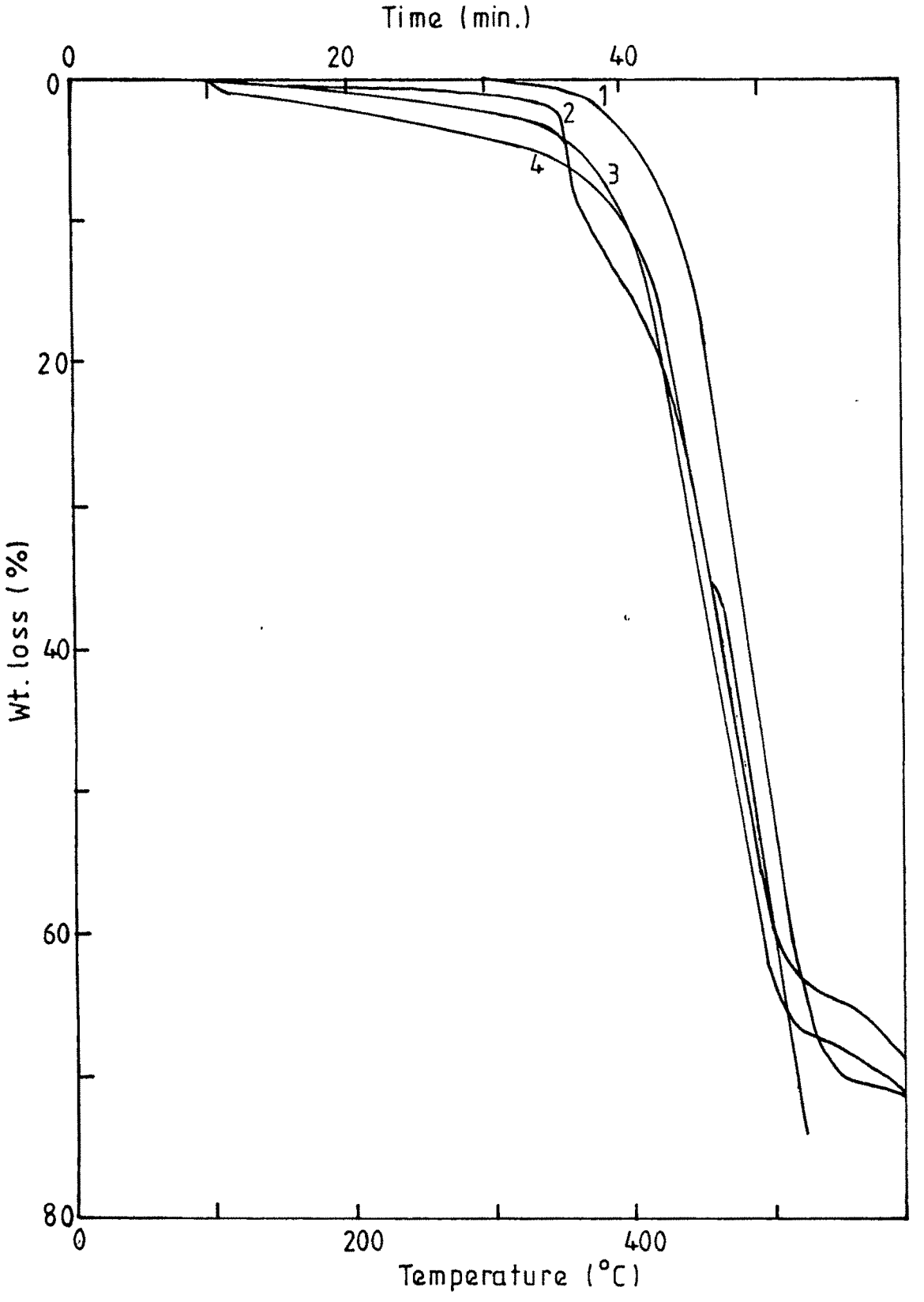

Fig. 3.22 Thermogravimetric curves of (1) 14PPd(II)EDTA (2) P(S-DVB) 14% cross-linked (3) 14PRu(III)Salen (4) 14PPd(II)Salen

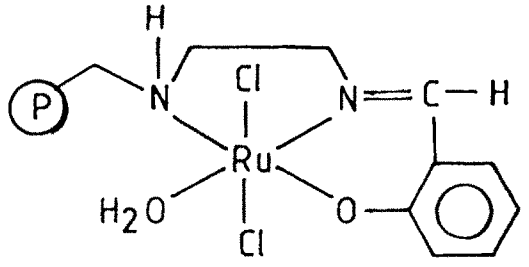

I

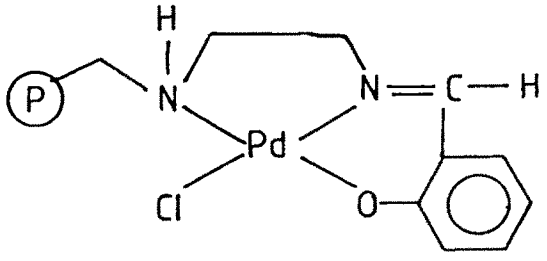

II

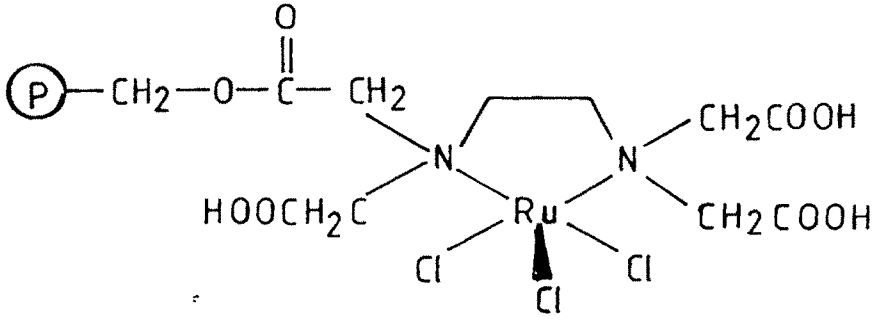

III

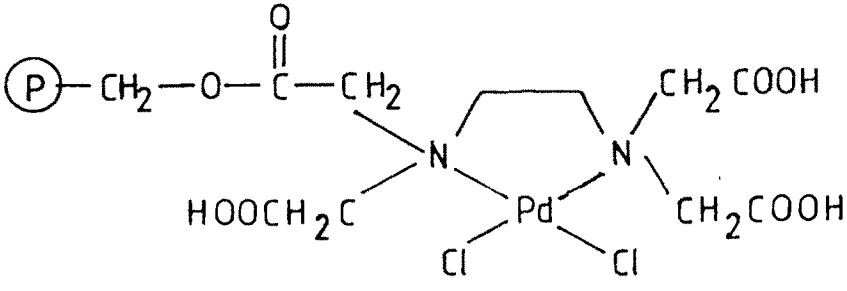

IV

SCHEME 3.1

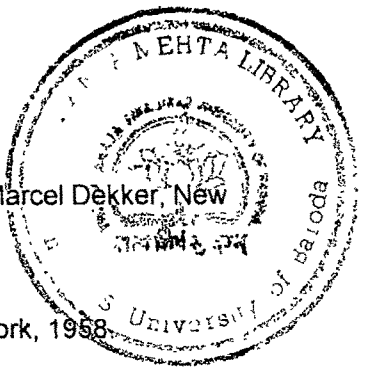

3.9 References

1. F. Delanny (Ed.) Characterization of heterogeneous catalysts, Marcel Dekker, New York, 1984
2. R Kunin, Ion Exchange Resins, John Wiley & Sons Ltd. New York, 1958.
3 C.N Shatterfield, Heterogeneous catalysis in industrial practice, McGraw Hill Inc , New York, 1993.
4. D.T.Gokak, B.V.Kamath and R.N Ram, J. Appl. Polymer Sci., **35**, 1523, 1988.
5. D.T.Gokak, B.V.Kamath and R N.Ram, Reactive Polymers, **10**, 37, 1989
6. J.N.Shah and R.N.Ram, J. Mol. Catal , **77**, 235, 1992
7. T. Teranishi and N. Toshima, J Chem Soc Dalton Trans. 2967, 1994.
8 F.R.Hartley, Supported Metal Complexes, D. Reidel, Dordrecht, 1985
9. H J.Mencer and Z. Gomzi, European Polymer J., **30**, 33, 1994.
10 B Erman and P.J.Flory, Macromolecules, 19, 2342, 1986.
11. G. Kortum, Reflectance Spectroscopy, Principles, Methods and Application, Springer-Verlag, Berlin, 1969.
11a R.P.Griffiths and J.A.Dettaseth, Fourier Transform Infrared Spectrometry, Wiley Inter Science, New York, 1986.
12. K. Siegbahn, C. Nordling, A. Fahlman, R Nordberg, K. Hamrin, J. Hedman, G Johansson, T. Bergmark, S.E. Karlsson, I Lindgren and B. Lindberg, ESCA: Atomic, Molecular and Solid State Structure studied by means of Electron Spectroscopy, Nova Acta Regiae Soc Sci Uppsaliensis, Ser. IV, Vol 20.
13 M.M.Taquikhan, S.A.Samad and M.R.H.Siddiqui, J Mol Catal , **50**, 97, 1989.
14. R Xavier and V. Mahadevan, J Polymer Science Part A: Polymer Chemistry, **30**, 2665, 1992.

15. J. Reed, P. Eisenberger, B.K.Teo and B.M.Kincaid, J. Am Chem Soc., **100**, 2375, 1978.

16. A.I.Kokorin and K.I.Zamaraev, Proc. 17th Int. Coord. Chem. Conf. Hamburg, 238, 1976.

17. R.S.Drago, J. Gaul, A. Zombeck and D.K.Straub, J. Amer. Chem Soc. **102(3),** 1033, 1980.

18. Y. Chimura, M. Beppu, S Yoshida and K. Tarama, Bull. Chem Soc Japan, **50**, 691, 1977

19. S.Sasaki, Y. Yanase, N. Hagiwara, T. Takeshila, H. Naganuma, A Ohyoshi and K. Ohkubo, J. Phys. Chem. Soc , **86**, 1038, 1982.

20. M.M.Taqui Khan, D. Srinivas, R.I.Kureshy and N.H.Khan, Inorg. Chem., **29**, 2320, 1990.

21. N.L.Holy, J. Org. Chem., **44**, 239, 1979.